

## Magnetic separation and characterization of vivianite from digested sewage sludge

Prot, T.; Nguyen, V. H.; Wilfert, P.; Dugulan, A. I.; Goubitz, K.; De Ridder, D. J.; Korving, L.; Rem, P.; Bouderbala, A.; Witkamp, G. J.

**DOI**

[10.1016/j.seppur.2019.05.057](https://doi.org/10.1016/j.seppur.2019.05.057)

**Publication date**

2019

**Document Version**

Accepted author manuscript

**Published in**

Separation and Purification Technology

**Citation (APA)**

Prot, T., Nguyen, V. H., Wilfert, P., Dugulan, A. I., Goubitz, K., De Ridder, D. J., Korving, L., Rem, P., Bouderbala, A., Witkamp, G. J., & van Loosdrecht, M. C. M. (2019). Magnetic separation and characterization of vivianite from digested sewage sludge. *Separation and Purification Technology*, 224, 564-579. <https://doi.org/10.1016/j.seppur.2019.05.057>

**Important note**

To cite this publication, please use the final published version (if applicable).  
Please check the document version above.

**Copyright**

Other than for strictly personal use, it is not permitted to download, forward or distribute the text or part of it, without the consent of the author(s) and/or copyright holder(s), unless the work is under an open content license such as Creative Commons.

**Takedown policy**

Please contact us and provide details if you believe this document breaches copyrights.  
We will remove access to the work immediately and investigate your claim.

See discussions, stats, and author profiles for this publication at: <https://www.researchgate.net/publication/333141214>

# Magnetic separation and characterization of vivianite from digested sewage sludge

Article in Separation and Purification Technology · May 2019

DOI: 10.1016/j.seppur.2019.05.057

CITATION

1

READS

274

11 authors, including:



**Thomas Prot**

Delft University of Technology

2 PUBLICATIONS 13 CITATIONS

[SEE PROFILE](#)



**Philipp Wilfert**

IPP - Kiel

11 PUBLICATIONS 121 CITATIONS

[SEE PROFILE](#)



**Kees Goubitz**

Delft University of Technology

265 PUBLICATIONS 5,075 CITATIONS

[SEE PROFILE](#)



**Leon Korving**

Wetsus

22 PUBLICATIONS 168 CITATIONS

[SEE PROFILE](#)

Some of the authors of this publication are also working on these related projects:



Biofilm Reactor Technology and Design [View project](#)



IWA Biofilms: Granular Sludge Conference 2018 [View project](#)

## Accepted Manuscript

Magnetic separation and characterization of vivianite from digested sewage sludge

T. Prot, V.H. Nguyen, P. Wilfert, A.I. Dugulan, K. Goubitz, D.J. De Ridder, L. Korving, P. Rem, A. Bouderbala, G.J. Witkamp, M.C.M. van Loosdrecht

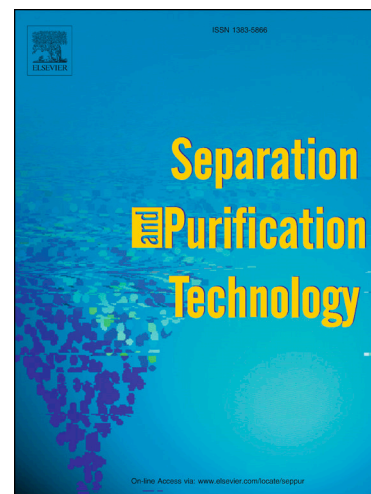
PII: S1383-5866(19)30430-7  
DOI: <https://doi.org/10.1016/j.seppur.2019.05.057>  
Reference: SEPPUR 15615

To appear in: *Separation and Purification Technology*

Received Date: 1 February 2019  
Revised Date: 15 May 2019  
Accepted Date: 15 May 2019

Please cite this article as: T. Prot, V.H. Nguyen, P. Wilfert, A.I. Dugulan, K. Goubitz, D.J. De Ridder, L. Korving, P. Rem, A. Bouderbala, G.J. Witkamp, M.C.M. van Loosdrecht, Magnetic separation and characterization of vivianite from digested sewage sludge, *Separation and Purification Technology* (2019), doi: <https://doi.org/10.1016/j.seppur.2019.05.057>

This is a PDF file of an unedited manuscript that has been accepted for publication. As a service to our customers we are providing this early version of the manuscript. The manuscript will undergo copyediting, typesetting, and review of the resulting proof before it is published in its final form. Please note that during the production process errors may be discovered which could affect the content, and all legal disclaimers that apply to the journal pertain.



**Magnetic separation and characterization of vivianite from digested sewage sludge**

T. Prot<sup>a,b</sup>, V.H. Nguyen<sup>a</sup>, P. Wilfert<sup>a,b</sup>, A.I. Dugulan<sup>c</sup>, K. Goubitz<sup>c</sup>, D.J. De Ridder<sup>d</sup>, L. Korving<sup>a,\*</sup>, P. Rem<sup>e</sup>, A. Bouderbala<sup>a</sup>, G.J. Witkamp<sup>b,f</sup> and M.C.M. van Loosdrecht<sup>b</sup>

<sup>a</sup>Wetsus, European Centre Of Excellence for Sustainable Water Technology, Oostergoweg 7, 8911 MA, Leeuwarden, The Netherlands

<sup>b</sup>Dept. Biotechnology, Delft University of Technology, Van der Maasweg 9, 2629 HZ Delft, The Netherlands

<sup>c</sup>Fundamental Aspects Mat & Energy Group, Delft University of Technology, Mekelweg 15, 2629 JB Delft, The Netherlands

<sup>d</sup>Sanitary Engineering, Delft University of Technology, Stevinweg 1, 2628 CN Delft, The Netherlands

<sup>e</sup>Resources and Recycling, Delft University of Technology, Stevinweg 1, 2628 CN Delft, The Netherlands

<sup>f</sup>Currently at King Abdullah University of Science and Technology (KAUST), Water Desalination and Reuse Center (WDRC), Division of Biological and Environmental Science and Engineering (BESE), Thuwal, 23955-6900, Saudi Arabia.

**\*Corresponding author: Phone: +31-58-2843160; e-mail: Leon.Korving@Wetsus.nl**

Keywords:

High gradient magnetic separation, Phosphorus recovery, XRD, Mössbauer spectroscopy, Heavy metals, Fertilizer

## Abstract

To prevent eutrophication of surface water, phosphate needs to be removed from sewage. Iron (Fe) dosing is commonly used to achieve this goal either as the main strategy or in support of biological removal. Vivianite ( $\text{Fe(II)}_3(\text{PO}_4)_2 \cdot 8\text{H}_2\text{O}$ ) plays a crucial role in capturing the phosphate, and if enough iron is present in the sludge after anaerobic digestion, 70 to 90% of total phosphorus (P) can be bound in vivianite. Based on its paramagnetism and inspired by technologies used in the mining industry, a magnetic separation procedure has been developed. Two digested sludges from sewage treatment plants using Chemical Phosphorus Removal were processed with a lab-scale Jones magnetic separator with an emphasis on the characterization of the recovered vivianite and the P-rich caustic solution. The recovered fractions were analyzed with various analytical techniques (e.g., ICP-OES, TG-DSC-MS, XRD and Mössbauer spectroscopy). The magnetic separation showed a concentration factor for phosphorus and iron of 2-3. The separated fractions consist of 52% to 62% of vivianite, 20% of organic matter, less than 10% of quartz and a small quantity of siderite. More than 80% of the P in the recovered vivianite mixture can be released and thus recovered via an alkaline treatment while the resulting iron oxide has the potential to be reused. Moreover, the trace elements in the P-rich caustic solution meet the future legislation for recovered phosphorus salts and are comparable to the usual content in Phosphate rock. The efficiency of the magnetic separation and the advantages of its implementation in WWTP are also discussed in this paper.

## 1. Introduction

Phosphorus is an essential element for life and is responsible for various functions in both humans and plants. Particularly for plants, it is a major nutrient and hence often spread onto soils in the form of phosphate fertilizer (Childers et al., 2011). The source for the phosphate in fertilizer is primarily from mining phosphate rock. This process is environmentally unfriendly, and the resources are becoming depleted whereas human's demand is increasing due to the rise of the population (Ridder et al., 2012). In parallel with being a necessary nutrient, phosphorus can also cause eutrophication if released in excess into water bodies, obliging Waste Water Treatment Plants (WWTPs) to remove it before discharging the effluents in natural streams. (Yang et al., 2008).

Currently, there are two main methods for advanced phosphorus removal in treatment plants: enhanced biological phosphorus removal (EBPR) and Chemical Phosphorus Removal (CPR). Iron is usually dosed in CPR mainly to remove the phosphorus but it also helps controlling the sulfide production and acts as a coagulant to facilitate sludge dewatering while being a cost-effective chemical. Furthermore, iron can already be present in the influent wastewater depending on its origin, meaning that P could already be partially bound to iron before the dosing step. Iron can also enhance the flocculation/coagulation of suspended particles in wastewater and thereby play a key role in future energy producing WWTP's (Wilfert et al., 2015).

It is estimated that 370 kton of phosphorus per year ends up in the sludge of the European WWTP's (Van Dijk, 2016). By utilizing this resource, up to 20-30% of Europe's fertilizer demand could be met (Schoumans, 2015). Hence, various technologies have been developed to serve this purpose, ranging from the direct use of sewage sludge on farmland to more advanced methods such as recovery from incinerated sewage sludge ash or recovery as struvite (Egle et al. 2016). There have not been many technologies proposed serving treatment

plants using CPR without the requirements for incineration. Incineration is often disapproved by the public and capital intensive as it requires expensive infrastructures.

In WWTP's dosing iron, several researchers reported the presence of the iron phosphate mineral vivianite ( $\text{Fe}_3(\text{PO}_4)_2 \cdot 8\text{H}_2\text{O}$ ). Frossard et al. 1997 discovered sand-sized to silt-sized vivianite in sludge while Seitz et al. 1973 observed it in dried sewage sludge. Nriagu and Dell 1974 evaluated that vivianite was the most thermodynamically stable FeP mineral in reductive environments, such as in sediments and sludge. More importantly, vivianite should form preferably over struvite during sludge digestion according to thermodynamic evaluations. Wilfert et al. 2016 observed this in two WWTP's where vivianite was found as the dominant FeP mineral in the digested sludge. In line with the findings of Poffet et al. 2008, this study also showed that Fe(III) compounds are reduced and transformed to vivianite in the activated sludge tanks even though Fe(III) was dosed. Additionally, Wilfert et al. 2018 suggested that after digestion between 70-90% of the total amount of P present in sludge can be bound to vivianite provided the dosing of iron is high enough.

With such a high fraction of P potentially present as vivianite, there is an opportunity to recover P from sludge through extraction of vivianite. It is especially interesting considering that only 10-50% of the total P in the influent can be recovered via struvite precipitation (Cornel and Schaum, 2009). Interestingly, vivianite is a paramagnetic mineral with a magnetic susceptibility varying from 0.8 to  $1.7 \cdot 10^{-6} \text{ m}^3/\text{kg}$  (Minyuk et al. 2013). Apart from some other Fe bearing species, vivianite is the only main paramagnetic compound in sludge. Magnetic separation would, therefore, provide a selective way to recover vivianite from sludge.

Seitz et al. 1973, already designed an experimental set-up to separate vivianite from dried sludge powder using magnetic attraction. There are also other devices from the mining industry like the Frantz separator that were used to extract magnetic fractions from streams but never tested to extract vivianite from sludge. These separators can only work with dry

materials and the separation of vivianite from sludge was not achieved with high efficiency (Bouderbala, 2016). Another device having the potential for this extraction process is the Jones separator, a high-intensity magnetic separator that can be used directly with wet sludge (Wills and Napier-munn, 2006). In this study, a device mimicking the working mechanism of the Jones separator was used to extract vivianite from sludge. The objective of this study was to provide the proof of principle that this technique can work and to investigate the composition of the extracted fraction. The magnetic separation of ferrite sludge from wastewater has already been studied earlier (Barrado et al. 1999) but is different from the technique studied here. Vivianite is paramagnetic and not ferromagnetic which makes its separation more challenging.

## **2. Materials and methods**



### 2.1. WWTP's and sample handling

For this research, digested sludges from 2 WWTP's have been used. One was sampled in Dokhaven (The Netherlands) and the other in Espoo (Finland). Both plants rely on CPR by dosing iron salts in different molar ratios to phosphate, which has an impact on the quantity of vivianite formed. After sampling, the sludges were kept in polyethylene bottles of 1L and stored in a 4°C fridge. Before any tests or analyses, the sludges were sieved with a 1 mm sieve to remove any large particles in the sludge. No particular precautions were taken to maintain anaerobicity of the feed samples considering that the sludge buffers oxygen and oxidation of vivianite should be slow in these conditions. A relatively pure (~ 95 % as determined with ICP-OES), vivianite scaling found in a heat exchanger from the WWTP of Venlo (The Netherlands) has been used as comparison during the study. More information about the sieved and non-sieved sludges can be found in Appendix A.

### 2.2. Magnetic separation and P release

#### *2.2.1 Definitions*

In this study, the initial mix from which the product is extracted is called the feed. The magnetic fraction containing the vivianite is the concentrate, while the non-wanted part is the tailing. The grade is the purity of the concentrate in terms of dry weight, and the recovery expresses the amount of a compound ending up in the concentrate compared to its quantity in the feed. The yield is defined as the quantity of concentrate compared to the feed in term of dry weight.

#### *2.2.2. Device description*

A lab-scale replicate of the separator ( $\mu$ -Jones) has been designed to investigate the application of this system to sludge. The  $\mu$ -Jones consists of two steel plates with seven vertical 4 cm-high/1.5 mm long teeth. The ridges are 2 mm away from each other and made magnetic with 2\*3 Nd-Fe-B permanent magnets of ~1.3 T (creating a magnetic field of ~1.3 T

on the ridge and  $\sim 0.3$  T in-between the teeth). The  $\mu$ -Jones is put in water until the teeth are entirely submerged to increase the contact time between the teeth and the sludge. An aluminum tray was designed to collect the solids as soon as they are released from the teeth. Further information about the working principle of a full-scale Jones separator can be found in Wills and Napier-munn, 2006.

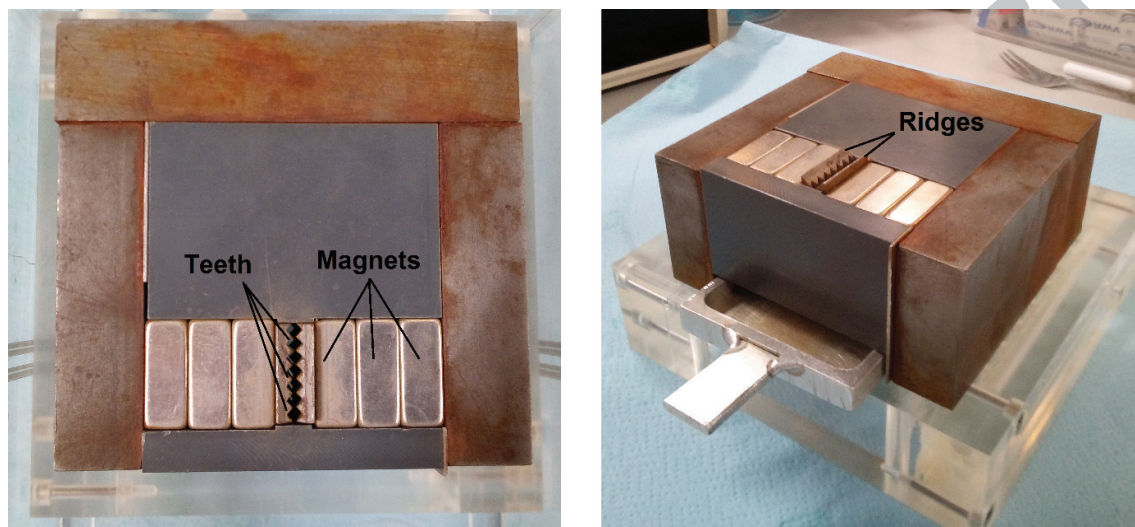


Figure 1:  $\mu$ -Jones top view (left) and side view (right)

### 2.2.3. Separation protocol

The sludge is continuously mixed for homogenization, and 20 mL/min are pumped on the teeth (Appendix B). The sludge from Finland was pumped for 30 seconds and the sludge from the Netherlands 45 seconds to obtain a similar quantity of concentrate because the amount of iron in the Finish sludge is higher. To wash away a maximum of non-magnetic residues stuck in the teeth (mainly organic matter), Milli-Q water (MQW) is pumped at 20 mL/min for 30 seconds. Finally, the  $\mu$ -Jones is removed from the water, and a stronger flow of MQW is sent through the teeth with a squeeze bottle to free all the material attached to the ridges.

As a post-treatment, the wet concentrate was introduced in 50 mL tubes to be centrifuged at 3750 rpm for 30 min. The pellets were then vacuum-dried at 30°C for 1-2 days. Around 250

mL (Finnish) and 500 mL (Dutch) of sieved sludge was necessary to separate 1 g of dried material. Feed samples were directly poured into a petri dish after sieving and vacuum dried at 30°C. All the materials (including the scaling) were then ground and stored in 15 mL plastic tubes without precaution toward exposure to oxygen or light. Once extracted from the sludge, vivianite is not protected anymore and can easily be oxidized (McCammon et al. 1980, Čermáková et al. 2013).

#### *2.2.4. Release of phosphorus from vivianite*

An alkaline treatment was used to release P from vivianite. 20 mg of concentrate was introduced in 10 mL of Ultratrace water (Sigma-Aldrich) under stirring, and 0.2 mL of 7.5 M ultratrace NaOH was added giving an OH<sup>-</sup>/Fe molar ratio excess of 5 - 10. The release solution is let to stir for 2h to be sure that the reaction is over. A change of color can be observed from transparent to the characteristic rust brown of Fe(OH)<sub>3</sub>. The precipitates were removed by 0.45µm filtration, and the filtrate was analyzed for elemental composition.

### 2.3. Analyses

#### *2.3.1 XRD*

The sample was filled in a 0.7 mm glass capillary and tamped so the solid settles. No precautions toward oxygen-free conditions have been taken. Just before measurement the capillaries were sealed with a burner and mounted in a sample holder. The device used was a PANalytical X'Pert PRO diffractometer with Cu-Kα radiation (5-80 °2θ, step size 0.008°). The fitting was realized with the software Origin Pro 9.

#### *2.3.2. SEM-EDX*

The apparatus is a JEOL JSM-6480 LV scanning electron microscope (SEM) equipped with an Oxford Instruments x-act SDD energy dispersive x-ray (EDX) spectrometer. The accelerating voltage used is 15.00 kV for a working distance of 10 mm. A 10 nm-layer of gold

is deposited on the sample with a JEOL JFC-1200 fine coater to make the surface electrically conductive. The software used are JEOL SEM Control User Interface for the SEM and Oxford Instruments Aztec for the EDX data processing.

### *2.3.3. Mössbauer spectroscopy*

The sample weight was adjusted to have 15 mg of Fe/cm<sup>2</sup>. Transmission <sup>57</sup>Fe Mössbauer absorption spectra were collected at 300 K and 77 K with a conventional constant-acceleration spectrometer using a <sup>57</sup>Co (Rh) source. Velocity calibration was carried out using an  $\alpha$ -Fe foil. The Mössbauer spectra were fitted using the Mosswin 4.0 program (Klencsár 1997).

### *2.3.4. TG-DSC-MS*

To evaluate the vivianite and the organic share in the samples, Thermo Gravimetry equipped with Differential Scanning Calorimetry, and a Mass Spectrometer (TG-DSC-MS) were used. The apparatus is a STA 449 F3 Jupiter for the simultaneous TG-DTA/DSC and QMS 403C Aëolos for the MS detector, both from NETZSCH Gerätebau GmbH. 40mg of sample is introduced in the oven which follows a continuous heating ramp of 10°C/min from 40°C until 550°C, under Argon atmosphere.

### *2.3.6. Digestion*

All the solid samples have been destroyed by microwave digestion to perform liquid analyses. The digestion takes place in an Ethos Easy from Milestone with an SK-15 High-Pressure Rotor. 10 mg of solid are introduced in a Teflon vessel in which 10 mL of ultrapure HNO<sub>3</sub> (64.5 – 70.5% from VWR Chemicals) is poured. The digester is set to reach 200 °C in 15 min, run at this temperature for 15 min and to cool down for 1h.

### 2.3.7. ICP-OES/MS

The elemental composition was measured via Inductively Coupled Plasma (Perkin Elmer, type Optima 5300 DV) with an Optical Emission Spectroscopy as detector (ICP-OES). The device was equipped with an Autosampler, Perkin Elmer, type ESI-SC-4 DX fast, and the data were processed with the software Perkin Elmer WinLab32. The rinse and internal standard solution were respectively 2% of HNO<sub>3</sub> and 10 mg/L of Yttrium.

ICP-OES doesn't allow to determine concentrations < 0.05ppm, so another ICP equipped with a Mass Spectrometer detector (ICP-MS) was also used. The device is a PlasmaQuant MS from Analytik-Jena and was used with three different analytical methods, depending on the element studied: with He (120 mL/min), with H<sub>2</sub> (80 mL/min) or without gas (ng). Y and In were used as internal standard in both gas mode whereas Sc and Y were used in no gas mode.

The samples from the P release experiments weren't digested before analysis but only filtered with a 0.45µm filter to remove the precipitates. More details about the ICP-MS method can be found in Appendix D.

## 3. Results

The magnetic separation of vivianite from digested sludge was performed, and the feeds and concentrates were analyzed to evaluate the separation. A relatively pure vivianite scaling sample from a WWTP plant in Venlo was used as a reference material. The names and description of the samples are presented in Table 1.

| Sample name | Description  |
|-------------|--|
| Feed NL     | Sieved digested sludge from Dokhaven (Netherlands) with a molar Fe/P ratio of 0.99 |
| Feed FI     | Sieved digested sludge from Espoo (Finland) with a molar Fe/P ratio of 2.19        |

|          |  |
|----------|--|
| Conc. NL | Magnetic fraction (concentrate) obtained from the processing of Feed NL  |
| Conc. FI | Magnetic fraction (concentrate) obtained from the processing of Feed FI  |
| Scaling  | Vivianite scaling of a purity >95% of vivianite harvested in Venlo (Netherlands).<br>This scaling is used as a reference for “pure” vivianite produced in sewage sludge. |

Table 1: Sample names and description

### 3.1. Solid analysis

#### 3.1.1. XRD

Vivianite was detected in all five samples described in Table 1 and was the only crystalline phase observed in all cases except for Feed NL (presence of quartz detected). While all the peaks could be assigned in the diffractograms obtained for the scaling and Conc. FI, one, three and four peaks remain unidentified for Conc. NL, Feed NL, and Feed FI, respectively. The bump between 15-40° that is usually considered to be amorphous material is absent for the concentrates and the scaling. The diffractogram can be found in Appendix F.

#### 3.1.2. SEM-EDX

SEM-EDX showed that Fe and P were not homogeneously distributed but clustered in specific overlapping places presenting sheet or needle-shaped crystals (5–15  $\mu\text{m}$ ) agglomerated into bigger particles (30-100  $\mu\text{m}$ ) (Figure 2). All the particles had a Fe/P ratio of 1.2-1.9, in the range of the one of vivianite (Table 2). Mg, Ca and Al were homogeneously distributed in the sample while S and Si were forming small clusters.

|                  | Scaling | Feed NL | Feed FI | Conc. NL | Conc. FI |
|------------------|---------|---------|---------|----------|----------|
| Molar Fe/P ratio | 1.8     | 1.2     | 1.6     | 1.4      | 1.9      |

Table 2: Molar ratio of the Fe/P overlapping particles found in the samples (EDX results)

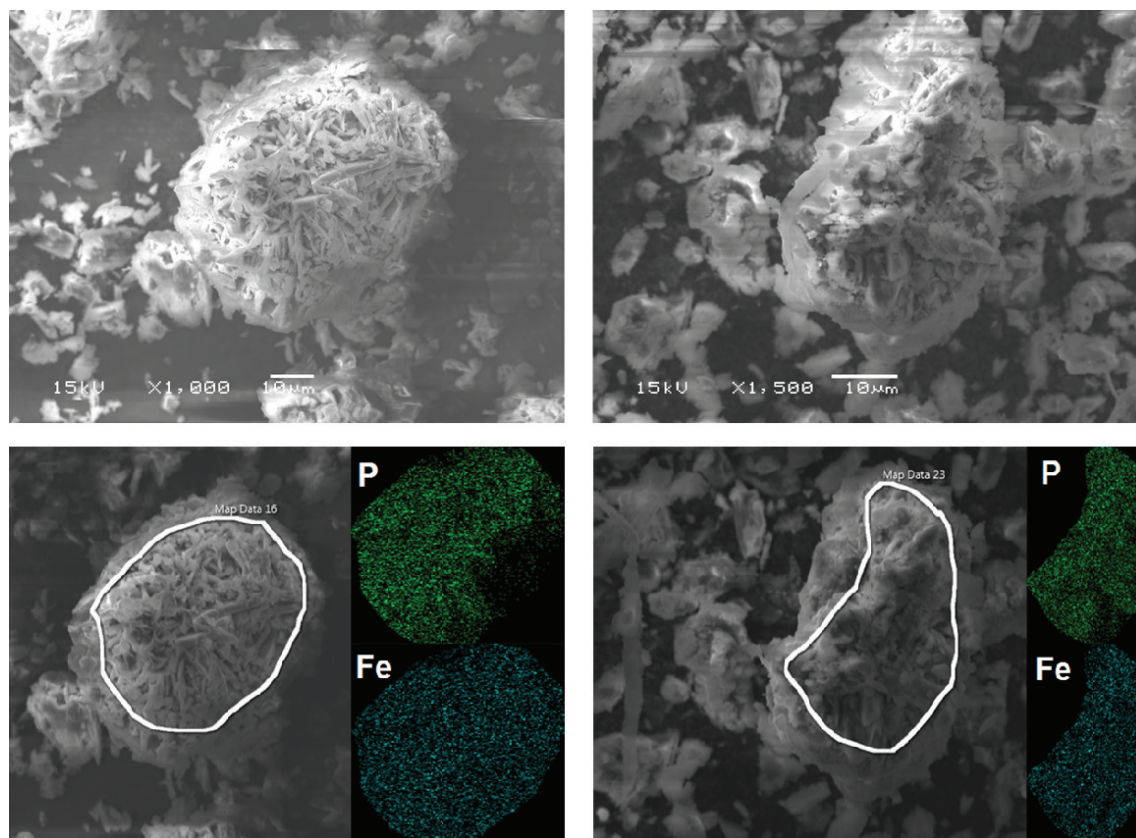


Figure 2: SEM pictures (top) and corresponding EDX maps (bottom) of the concentrates from Finland (left) and the Netherlands (right)

### 3.1.3. Mössbauer spectroscopy

In Table 3,  $\text{Fe}^{3+}$  stands for oxidized iron either in the vivianite structure or as another Fe (III) species.  $\text{Fe}^{\text{II}}$  stands for low-spin iron compounds (typically pyrite). In the crystalline structure of vivianite,  $\text{Fe}^{2+}$  ions can occupy three positions, always in the center of octahedrons formed by water molecules and oxygen atoms. Two positions are equivalent and named  $\text{Fe}^{2+}$  Vivianite B in Table 3 while the third is unique and called  $\text{Fe}^{2+}$  Vivianite A (Grodzicki and Amthauer 2000). Other crystalline Fe phases weren't identified.

| <i>Sample</i> | <i>T</i><br>(K) | <i>IS</i><br>(mm·s <sup>-1</sup> ) | <i>QS</i><br>(mm·s <sup>-1</sup> ) | <i>Hyperfine</i><br><i>field (T)</i> | <i>Γ</i><br>(mm·s <sup>-1</sup> ) | <i>Phase</i>                       | <i>Spectral</i><br><i>contribution</i><br><i>n (%)</i> |
|---------------|-----------------|------------------------------------|------------------------------------|--------------------------------------|-----------------------------------|------------------------------------|--|
| Scaling       | 300             | 0.33                               | 0.88                               | -                                    | 0.54                              | Fe <sup>3+</sup>                   | 32   |
|               |                 | 1.22                               | 2.40                               | -                                    | 0.36                              | Fe <sup>2+</sup> Vivianite A       | 27   |
|               |                 | 1.22                               | 2.96                               | -                                    | 0.36                              | Fe <sup>2+</sup> Vivianite B       | 41   |
| NL conc.      | 300             | 0.34                               | 0.88                               | -                                    | 0.49                              | Fe <sup>3+</sup> /Fe <sup>II</sup> | 35   |
|               |                 | 1.26                               | 2.35                               | -                                    | 0.39                              | Fe <sup>2+</sup> Vivianite A       | 25   |
|               |                 | 1.23                               | 2.95                               | -                                    | 0.39                              | Fe <sup>2+</sup> Vivianite B       | 40   |
| FI conc.      | 300             | 0.38                               | 0.82                               | -                                    | 0.53                              | Fe <sup>3+</sup> /Fe <sup>II</sup> | 70   |
|               |                 | 1.25                               | 2.09                               | -                                    | 0.39                              | Fe <sup>2+</sup> Vivianite A       | 16   |
|               |                 | 1.19                               | 2.95                               | -                                    | 0.39                              | Fe <sup>2+</sup> Vivianite B       | 14   |
| NL feed       | 300             | 0.36                               | 0.85                               | -                                    | 0.53                              | Fe <sup>3+</sup> /Fe <sup>II</sup> | 66   |
|               |                 | 1.27                               | 2.31                               | -                                    | 0.31                              | Fe <sup>2+</sup> Vivianite A       | 13   |
|               |                 | 1.22                               | 2.97                               | -                                    | 0.31                              | Fe <sup>2+</sup> Vivianite B       | 21   |
| FI feed       | 300             | 0.38                               | 0.87                               | -                                    | 0.57                              | Fe <sup>3+</sup> /Fe <sup>II</sup> | 61   |
|               |                 | 1.21                               | 1.99                               | -                                    | 0.43                              | Fe <sup>2+</sup> Vivianite A       | 27   |
|               |                 | 1.14                               | 2.81                               | -                                    | 0.43                              | Fe <sup>2+</sup> Vivianite B       | 12   |

Table 3: Mössbauer data for the 5 samples at 300K



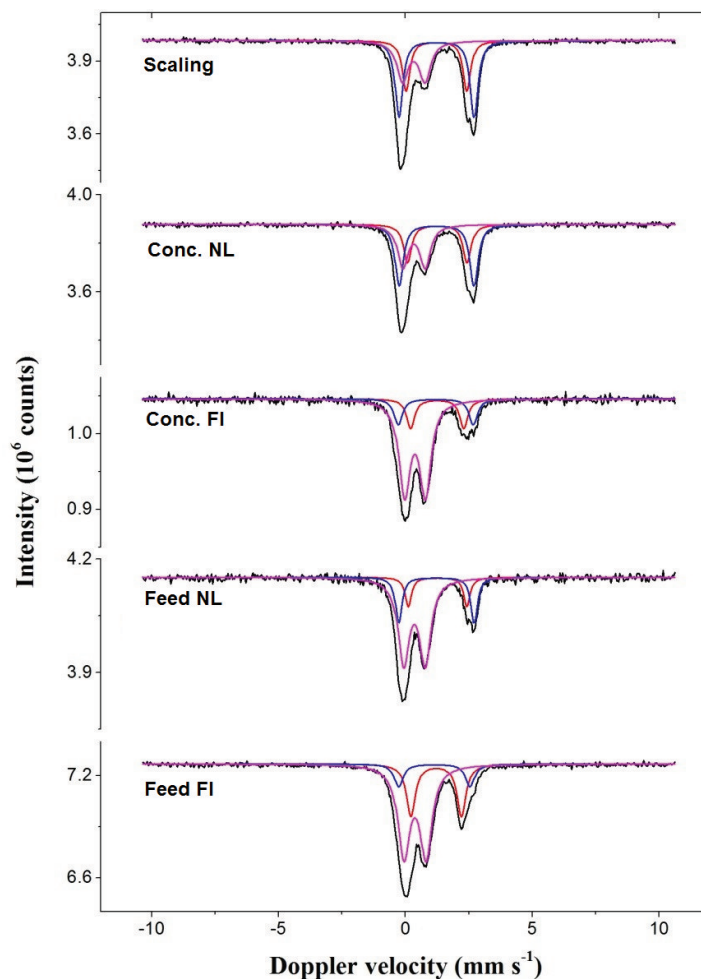


Figure 3: Mössbauer spectra obtained at 300K with the signal of  $Fe^{3+}/Fe^{II}$  in pink,  $Fe^{2+}$  Vivianite A in red,  $Fe^{2+}$  Vivianite B in blue and the sum of the spectrum in black.

#### 3.1.4. TG-DSC-MS

The TG analysis of the scaling presented a weight decrease of 25% before 200 °C while 5% is lost between 200 °C and 550 °C. The other samples presented two weight decreases, the first one being steeper for the concentrates than for feed samples. The temperature intervals for the loss of water and  $CO_2$  (blue and orange curves in Figure 4) are slightly different for each sample (Table 4). Based on the MS signal and the results for the scaling, the first weight decrease can be attributed to the evaporation or 7 of the 8  $H_2O$  of vivianite while the second

decrease should account for the last H<sub>2</sub>O, the organic fraction and other unidentified minor phases.

| Sample   | 1 <sup>st</sup> decrease (% of weight lost) | 2 <sup>nd</sup> decrease (% of weight lost) |
|----------|---|---|
| Scaling  | 25 (40-220 °C)                              | 5 (220-550°C)                               |
| Feed FI  | 10 (40-200 °C)                              | 36 (200-550°C)                              |
| Feed NL  | 12 (40-220 °C)                              | 40 (220-550°C)                              |
| Conc. FI | 14 (40-200 °C)                              | 23 (200-550°C)                              |
| Conc. NL | 17 (40-200 °C)                              | 20 (200-550°C)                              |

Table 4: Weight losses during the 1<sup>st</sup> and the 2<sup>nd</sup> decrease in TG analysis (after vacuum oven drying)

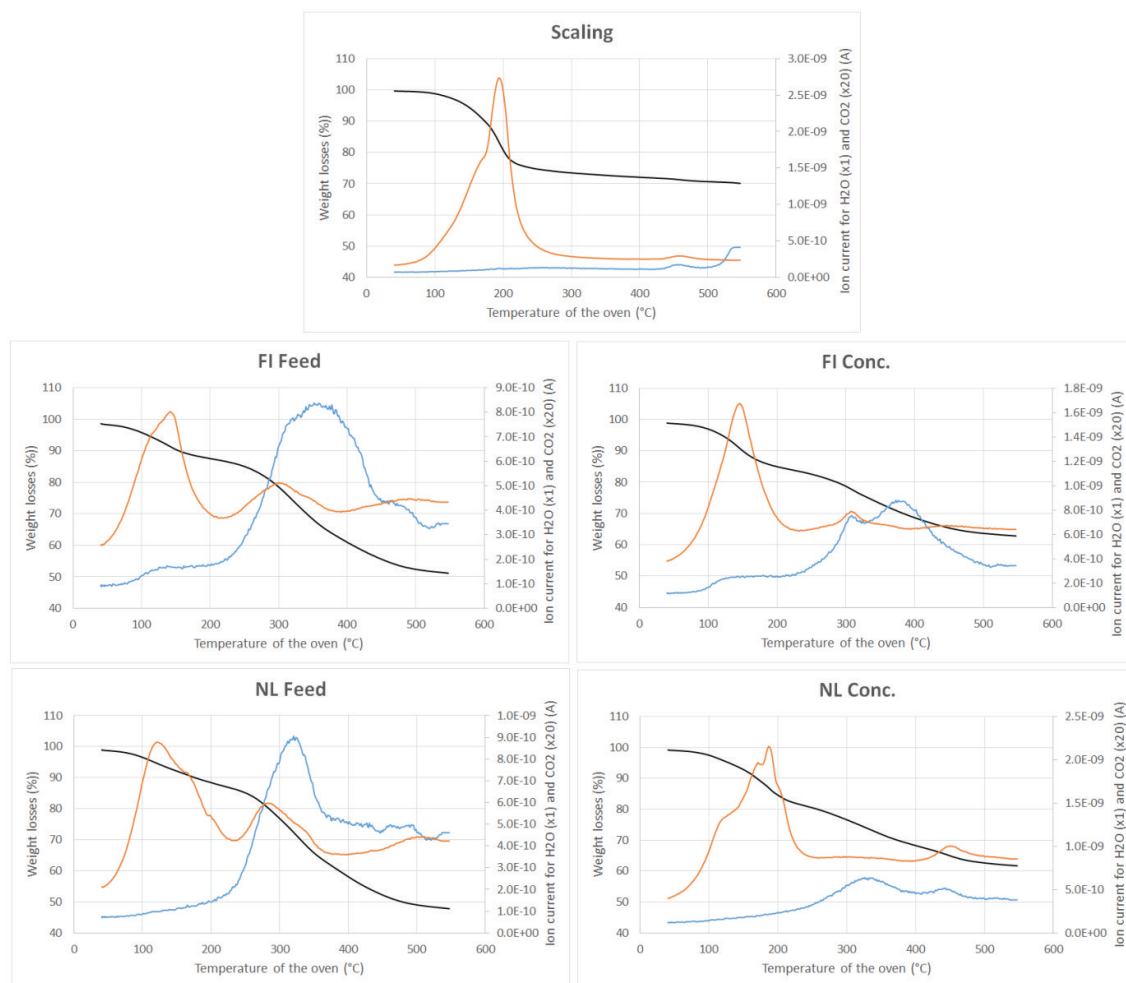


Figure 4: TG-DSC-MS spectra for the scaling, both feeds, and concentrates. In black the weight losses, in orange the Mass Detector signal for  $H_2O$  and in blue for  $CO_2$

### 3.2. Elemental composition: ICP-OES/MS

The elemental composition of all samples has been determined after microwave digestion. For both feeds, the major elements detected were Fe, P and Ca, with twice as much Fe in FI Feed than NL Feed due to the larger Fe dosing. The quantity of Fe and P increased by a factor 2-3 after separation while the other elements' share was reduced (Table 5).

| g/kg of dry matter | Fe             | P              | Ca             | Mg            | Al            | S             | K             | Zn           | Si            | Cu           | Na   | Mn           |
|--------------------|----------------|----------------|----------------|---------------|---------------|---------------|---------------|--------------|---------------|--------------|------|--------------|
| FI Feed            | 120.3<br>± 0.5 | 28.4<br>± 0.1  | 26.7<br>± 0.6  | 4.0<br>± 0.1  | 6.1<br>± 0.1  | 8.6<br>± 0.1  | 10.8<br>± 0.3 | 0.8*         | 7.9<br>± 0.1  | nd           | nd   | nd           |
| FI Conc.           | 236.2*         | 64.6<br>± 0.7  | 17.14<br>± 0.6 | 2.8<br>± 0.1  | 4.6<br>± 0.1  | 6.0<br>± 0.8  | 2.0*          | 0.5*         | 5.5<br>± 0.2  | 1.0*         | nd   | nd           |
| NL Feed            | 63.9<br>± 0.1  | 37.4<br>± 0.6  | 36.2<br>± 0.7  | 3.4<br>± 0.1  | 6.0<br>± 0.1  | 20.9<br>± 0.2 | 10.3<br>± 0.1 | 1.3<br>± 0.1 | 7.00<br>± 0.1 | 0.7<br>± 0.1 | 7.2* | nd           |
| NL Conc.           | 195.2*         | 77.21<br>± 0.8 | 20.0<br>± 0.4  | 7.50<br>± 0.1 | 4.62<br>± 0.1 | 9.6<br>± 0.4  | 1.8*          | 0.7*         | 5.56<br>± 0.1 | 0.7*         | nd   | 2.4*         |
| Scaling            | 308.0*         | 119.0 ±<br>2.2 | 9.5<br>± 0.5   | 10.8<br>± 0.1 | nd            | 1.70<br>± 0.8 | nd            | nd           | nd            | nd           | nd   | 3.0<br>± 0.1 |

Table 5: Elemental composition of the feeds, concentrates and scaling measured by ICP-OES

\* one of the duplicate is out of range (high or low)

nd: not detected because the concentration was below the LOQ of the device for both duplicates

ICP-MS was used in complement of ICP-OES to reach lower concentrations. The limit of quantification (LOQ) was established by setting a threshold of 20% to the relative standard deviation (RSD) of the calibration curve for each element (EPA publication SW-846). Only results above the LOQ are presented in Table 6. For these analyses the device encountered analytical problems measuring Si, S, K, Ca and Ti. As observed by ICP-OES, most elements are reduced in concentration after magnetic separation

| Sample   | Weight content (mg element/kg of dry matter) |               |               |              |      |                |                 |               |                |                 |                 |               |              |               |                |                |                 |               |               |
|----------|--|---------------|---------------|--------------|------|----------------|-----------------|---------------|----------------|-----------------|-----------------|---------------|--------------|---------------|----------------|----------------|-----------------|---------------|---------------|
|          | Cr   | As            | La            | Li           | Mg   | Al             | Mn              | Co            | Ni             | Cu              | Zn              | Mo            | Ag           | Sn            | Ba             | Pb             | Na              | Rb            | Ce            |
| FI Feed  | 33.1<br>± 0.6                                | 8.7<br>± 0.5  | 30.1<br>± 0.3 | 3.6<br>± 0.1 | >790 | >790           | 252.0<br>± 0.5  | 8.8<br>± 0.1  | 33.3<br>± 0.3  | 378.3<br>± 4.2  | 725.1<br>± 10.8 | 6.0<br>± 0.1  | 2.8<br>± 0.1 | 27.3<br>± 0.2 | 114.2<br>± 0.6 | 15.4<br>± 0.1  | >790            | 10.6<br>± 0.1 | 74.8<br>± 0.7 |
| FI Conc. | 25.1<br>± 0.5                                | 7.7<br>± 0.7  | 24.4<br>± 0.3 | 3.1<br>± 0.2 | >790 | >790           | 414.3<br>± 3.01 | 9.2<br>± 0.1  | 398.2<br>± 1.3 | >790            | 414.2<br>± 0.9  | 4.1<br>± 0.1  | nd           | 18.3<br>± 0.1 | 94.2<br>± 0.7  | 8.2<br>± 0.1   | nd              | 6.6<br>± 0.2  | 51.3<br>± 0.4 |
| NL Feed  | 50.7<br>± 0.7                                | 40.1<br>± 1.2 | 9.5<br>± 0.1  | 3.9<br>± 0.2 | >790 | >790           | 634.5<br>± 4.6  | 6.1<br>± 0.1  | 42.2<br>± 0.5  | 685.6<br>± 10.9 | >790            | 11.8<br>± 0.1 | 7.0<br>± 0.2 | 25.5<br>± 0.2 | 400.7<br>± 1.2 | 113.1<br>± 1.8 | >790            | 7.9<br>± 0.2  | 13.1<br>± 0.2 |
| NL Conc. | 59.7<br>± 1.7                                | 17.9<br>± 0.4 | 7.0<br>± 0.1  | 3.8<br>± 0.2 | >782 | >782           | >782            | 8.5<br>± 0.1  | 90.6<br>± 0.6  | 710.0<br>± 4.5  | 648.1<br>± 7.0  | 5.6<br>± 0.1  | 3.3<br>± 0.3 | 17.7<br>± 0.2 | 239.8<br>± 1.4 | 81.5<br>± 0.6  | 239.3<br>± 40.5 | 5.0<br>± 0.2  | 11.4<br>± 0.1 |
| Scaling  | nd   | nd            | nd            | nd           | >782 | 297.1<br>± 0.8 | >782            | 31.7<br>± 0.4 | 78.6<br>± 0.5  | 17.1<br>± 1.5   | 267.7<br>± 2.0  | nd            | nd           | nd            | nd             | 3.3<br>± 0.1   | nd              | nd            | nd            |

Table 6: Elemental composition of the feeds, concentrates and scaling measured by ICP-MS

nd: no data, meaning below LOQ for both replicates

After alkaline release of P from the concentrates and filtration, only 4 elements can be detected in the filtrate by ICP-OES (Table 7). This result is confirmed by the small number of elements detected by ICP-MS in further experiments (Table 8). The device encountered problems measuring Si, S, K, Ca and Ti for these measurements.

| Sample           | Weight content (g solubilized element/kg of dry matter) |              |             |       |
|------------------|---|--------------|-------------|-------|
|                  | Al  | P            | S           | Si    |
| FI Conc. release | 1.84 ± 0.12   | 59.67 ± 4.64 | 5.04 ± 0.68 | 0.96* |
| NL Conc. release | 1.73 ± 0.18   | 69.93 ± 5.54 | 6.70 ± 0.54 | nd    |

Table 7: Elemental composition of the release solution for both concentrates measured by ICP-OES

\* the second replicate is below the LOQ of the device

nd: no data, meaning below LOQ for both replicates

| Sample           | Weight content (mg solubilized element/kg dry matter) |                |                 |                  |                 |                |                 |                   |
|------------------|---|----------------|-----------------|------------------|-----------------|----------------|-----------------|-------------------|
|                  | As  | Mn             | Ni              | Cu               | Zn              | Mo             | Sn              | Fe                |
| FI Conc. release | 3.18<br>± 0.08  | 2.66<br>± 0.34 | 90.51<br>± 1.24 | 196.16<br>± 6.85 | 24.76<br>± 2.52 | 2.20<br>± 0.05 | 10.58<br>± 0.74 | 281.49<br>± 23.42 |
| NL Conc. release | 12.98<br>± 0.68                                       | 8.76<br>± 0.32 | 12.48<br>± 0.06 | 113.59<br>± 3.44 | 34.21<br>± 2.54 | 2.76<br>± 0.04 | 9.09<br>± 0.48  | 183.77<br>± 50.13 |

Table 8: Elemental composition of the release solution for both concentrates measured by ICP-MS

## Discussion

The objective of this project was to prove that magnetic extraction of vivianite from sludge is possible and selective by means of a lab scale magnetic separator that mimics the working principle of large scale wet magnetic separators. As a proof of concept study, a pure product rather than a high yield was sought in order to selectively extract vivianite to be able to study and understand how vivianite is present in digested sewage sludge. Three main points will be discussed in the following section:

- The magnetic separation performances
- The composition of the magnetic concentrate in terms of vivianite content and side products.
- The valorization possibilities of the concentrate with an emphasis on its transformation into a fertilizing material

The samples names and description are indicated in Table 1.

| % of dried matter | Vivianite  | Organics** | Quartz** |
|-------------------|------------|------------|----------|
| FI Feed           | 6.9 - 23.0 | 39 ± 2     | 8        |
| FI Conc.          | 52.3 ± 0.6 | 20 ± 2     | 8        |
| NL Feed           | 6.6 - 30.2 | 42 ± 2     | 4        |
| NL Conc.          | 62.5 ± 0.7 | 19 ± 2     | 7        |

*Table 9: Vivianite, organics and quartz content of the feeds and concentrates (processed data from Table 3, Table 4, Table 5 and Table)*

\* For the concentrates, the content has been determined with ICP-OES assuming that all the P is bound to vivianite which should be the major (if not the only) magnetic P-specie in the sample. For the Feeds, this hypothesis is not applicable considering the diversity of P compounds in sludge (CaP, organic P...). Therefore, a range is given with the minimum determined by Mössbauer and the maximum by ICP-OES.

\*\* Details of the determination of the content stand in Appendix C.

To evaluate the potential of the magnetic separation, it is interesting to compare the composition of the magnetic fraction to the digested sludge, before separation. The vivianite content in the magnetic concentrates was reliably estimated with ICP-OES and TG-DSC-MS (see further in the discussion). Mössbauer spectroscopy is unable to differentiate the fraction of oxidized vivianite from other Fe<sup>3+</sup> bearing compounds present in sludge. The samples were exposed to oxygen during the separation and sampling handling, resulting in some oxidation of the vivianite. Therefore, in this case, Mössbauer spectroscopy underestimated the vivianite content and gives the minimum rather than the exact content. Furthermore, the maximum vivianite content can be obtained by hypothesizing that all the P measured by ICP-OES in the samples are present as vivianite. A combination of Mössbauer spectroscopy and ICP-OES gives a range of vivianite content in the digested sludge (Table 9). Earlier, more detailed studies on the vivianite content of the same sludges (Wilfert et al. 2018) estimated the phosphorus present as vivianite at 65% and 85% of the total phosphorus (average value from their measurements) in NL Feed and FI Feed, respectively. Based on the elemental composition of these sludge in Table 5, the vivianite weight content can be estimated at 20 % for both sludges. This suggests that the magnetic separation concentrates the vivianite by a factor 2-3, which is promising at this stage. The magnetic separation also reduces the organic content from 40% to 20% (Table 9). The remaining could be the organic matter that seems to trap the vivianite crystals, as suggested by Figure 2 and Frossard et al. 1997. The persistence of quartz even after magnetic separation is surprising considering that quartz is not paramagnetic. It could act as nucleation center for vivianite, and may therefore be present in its structure, and be extracted with it.

| Sample   | Fe <sup>2+</sup> Vivianite A (%) | Fe <sup>2+</sup> Vivianite B (%) | Ratio B/A |
|----------|----------------------------------|----------------------------------|-----------|
| NL Conc. | 25                               | 40                               | 1.6       |
| FI Conc. | 9*                               | 14                               | 1.6       |
| NL Feed  | 13                               | 21                               | 1.6       |



|         |    |    |     |
|---------|----|----|-----|
| FI Feed | 7* | 12 | 1.7 |
|---------|----|----|-----|

Table 10: Spectral contribution of both  $Fe^{2+}$  sites of vivianite at 300K and site ratio (processed data from Table 3)

\* The QS of Vivianite A (Table 3) is lower than it should ( $\sim 2.1$  instead of  $\sim 2.4$  mm/s) for these samples indicating a probable interference with the siderite (QS  $\sim 1.8$  mm/s) present as well. Therefore, the contribution of siderite (calculated further in the discussion) is deducted from this signal, giving a spectral contribution of 9% (instead of 16%) and 7% (instead of 27%) for FI Conc. and FI Feed, respectively.

Since the concentration of heavy metals is relevant for the valorization of the magnetic concentrate, we studied the concentration factor of heavy metals during the separation. Our study shows that the magnetic separation reduces the heavy metal to phosphorus ratio (Appendix E). However, this is not the case for the cations Mn, Ni, Mg and Cu that remained similar or increased. The authors see two possible explanations for the persistence of these elements in the magnetic fraction: they could form other magnetic compounds than vivianite, or substitute  $Fe^{2+}$  in the structure of vivianite. Vivianite is known to have a structure allowing substitution of its  $Fe^{2+}$  atoms by other divalent cations (Rothe et al. 2016 and Taylor et al. 2008). At ambient temperature, 2  $Fe^{2+}$  occupy the 2 octahedral sites B while 1  $Fe^{2+}$  occupies the octahedral site A. Therefore, the ratio ( $Fe^{2+}$  Vivianite B /  $Fe^{2+}$  Vivianite A) given by Mössbauer should be 2 for pure vivianite (McCammon et al. 1980, Mori and Ito 1950). Divalent cations substitute preferentially in site B, decreasing this ratio (Manning et al. 1991). The samples have ratios  $< 2$  suggesting the presence of impurities (Table 10). This ratio is an interesting indicator to assess the purity of the vivianite, but oxidation of the mineral complicates the evaluation. Rouzies and Millet 1993 and McCammon et al. 1980 consider that oxidation happens preferentially in site A which should then increase the ratio. The antagonist effects of the oxidation and the impurities make a quantitative approach impossible in the case of samples that were exposed to air, as was the case in this study.

A deeper characterization of the magnetic fractions has been realized to assess the purity of the product. First of all, vivianite was clearly identified in the magnetic concentrates by Mössbauer spectroscopy and XRD. Crystals showing a Fe/P ratio close to 1.5 (as in pure vivianite) were also observed by SEM-EDX (Table 2). Moreover, the morphology of these crystal as on Figure 2 agrees with the sheet/needle-shaped appearance of vivianite already reported by several authors (Zelibor et al. 1988, Taylor et al. 2008).

| Content (weight % of dried matter) | Conc. NL       | Conc. FI         |
|------------------------------------|----------------|------------------|
| ICP-OES                            | $62.5 \pm 0.7$ | $52.3 \pm 0.6$   |
| TG-DSC-MS                          | $68 \pm 8$     | $56 \pm 8$       |
| Mössbauer                          | $38.4 \pm 0.9$ | $16.4 \pm 0.3^*$ |

Table 11: Vivianite content in the concentrates estimated with different analytical methods (processed data from Table 3, Table 4 and Table 5)

\* see explanation below Table 10

The quantification of vivianite is complicated and, therefore, ICP-OES, TG-DSC-MS and Mössbauer spectroscopy were used together to give the best result possible (Table 11). A first estimate of the vivianite content can be made based on the elemental composition (ICP-OES) by hypothesizing that all the phosphorus is bound to vivianite in these samples. It seems like a reasonable assumption since vivianite should be the major (if not the only) magnetic P-compound in sludge. Additionally, TG-DSC-MS was used. This method is based on the dehydration process of vivianite, that loses its 8 crystal water with temperature increase. The vivianite scaling used as reference for pure vivianite (Table 1) indicates that 7 of its 8 crystal water evaporate in the temperature range 40-200°C (Figure 4). The vivianite content in the concentrates is estimated by matching the weight decrease in this temperature range to the loss of 7 water molecules (Table 4). In complement, Mössbauer spectroscopy was used. It can detect the Fe<sup>2+</sup> ions of vivianite but is unable to quantify them after they oxidize to Fe<sup>3+</sup>, even

though they are still present in the structure of vivianite. This is because the signal of  $\text{Fe}^{3+}$  in vivianite overlaps with other oxidized Fe phases and low-spin iron like in pyrite (Nishihara, Y., & Ogawa, S. 1979) and cannot be isolated. Therefore, only the contribution of  $\text{Fe}^{2+}$  can be taken into account to estimate the vivianite content, this giving a conservative estimate for the vivianite content. No precaution toward oxidation has been taken during magnetic separation and sample handling, and therefore the  $\text{Fe}^{3+}$  content in any recovered vivianite will not be negligible explaining the low vivianite content obtained with Mössbauer in Table 11. ICP-OES and TG-DSC-MS seem fit to estimate the vivianite content in the magnetic fraction while Mössbauer spectroscopy requires extreme precaution toward oxidation to be reliable.

| Content (weight % of dried matter) | Organic matter* | $\text{FeCO}_3$ * | Quartz*   |
|------------------------------------|-----------------|-------------------|-----------|
| FI Conc.                           | $20 \pm 2$      | $3.33 \pm 0.16$   | $8 \pm 1$ |
| NL Conc.                           | $19 \pm 2$      | $0.26 \pm 0.02$   | $7 \pm 1$ |

Table 12: Organic matter,  $\text{FeCO}_3$  and quartz content measured in both magnetic concentrates

\* Details of the determination of the content is in Appendix C.

Vivianite accounts for 50-60% of the weight of the magnetic fractions, so 40-50% are left to determine. Organic matter, quartz and carbonates (likely to be siderite  $\text{FeCO}_3$ ) were also found and their estimated content are listed in Table 12. Organic matter has been quantified by TG-DSC-MS since it should lead to mass loss due to pyrolysis and gasification before  $550^\circ\text{C}$  (responsible for the second weight drop in Table 4). The quartz content was considered to be equal to the residue after microwave digestion. SEM EDX confirmed this residue contained mainly silica and oxygen. The carbonate quantity was estimated based on the  $\text{CO}_2$  release from the sample after acid addition to the sample. Methods and results are detailed in Appendix C.

The Fe content in the magnetic fraction is high compared to the phosphorus content (Table 5) and the presence of vivianite cannot alone explain it. Therefore, other Fe species must have been extracted together with vivianite. No other Fe compound was positively identified by XRD or Mössbauer, indicating a low content, a small size or/and an amorphous nature of these Fe compounds. The carbonates found in the magnetic fractions are likely to be  $\text{FeCO}_3$  (siderite) (Appendix C); not only is it a magnetic specie (Frederichs et al. 2003) but it is also the possible reason for the interference observed with Mössbauer spectroscopy (see explanation below Table 10). Pyrite, another magnetic compound, can potentially be present in the magnetic fraction and could account for 3-5% of the dried weight if we consider that the sulfur quantified by ICP-OES is present in the form  $\text{FeS}_2$ . SEM-EDX also revealed some Fe/S clusters (results not showed) which support this hypothesis. As mentioned above, pyrite is a low-spin Fe and cannot be distinguished from  $\text{Fe}^{3+}$  species by Mössbauer, explaining why it has not been identified with certainty. Other Fe-species like  $\text{FeOH}$ 's should be present in the magnetic fraction to account for the rest of  $\text{Fe}^{3+}$  detected by Mössbauer.

In conclusion, the magnetic fractions contain organic matter (20%), quartz (7-8%), pyrite (3-5%), siderite (0.3-3%) and other not identified compounds. Most importantly, the vivianite content is estimated to be around 50% of the concentrate, showing the feasibility to concentrate vivianite magnetically, albeit that further work needs to be done to improve the purity of the concentrate, and the yield.

Once vivianite is recovered from sludge, several valorizations may be foreseen. If a high-grade concentrate could be obtained, high-value applications could be considered. Using vivianite in art to create pigments or as a component in the lithium-ion batteries are two such high-value possibilities (Čermáková et al. 2013, Recham et al. 2009). Several studies have already investigated the direct use of vivianite as a slow P-release fertilizer and its advantage for Fe-poor soils (Fodoué et al. 2015, Rombolà et al. 2007). However, they were working

with natural vivianite and not vivianite from sewage, which might bear heavy metals, possibly limiting a direct use. On the other hand, their presence could also be beneficial for some plants requiring micronutrients like Cu or Zn.

If the purity of the concentrate is too low for direct application, a post-treatment is required to crack vivianite and recover the P and the Fe. With this objective, the magnetic concentrate was put in an alkaline solution (2.2.4. Release of phosphorus from vivianite) which broke down the vivianite, released P in solution, while Fe and the other heavy metal precipitated as hydroxides. The precipitates were filtered out and around 90% of the P from vivianite was recovered in the liquid fraction.

| Elements<br>(mg/kg of P)*        | As       | Cd      | Cr         | Cu         | Ni         | Pb       | Zn       |
|----------------------------------|----------|---------|------------|------------|------------|----------|----------|
| PFC 1(C)1**                      | 87       | 130     | 13         | 3921       | 649        | 104      | 9803     |
| P-rock***                        | 66 - 94  | 107-271 | 536 - 1993 | <1886      | < 186      | 50 - 100 | <1864    |
| P-rich solution<br>from NL Conc. | 186 ± 11 | < 195   | < 23       | 1631 ± 81  | 180 ± 19   | < 22     | 490 ± 28 |
| P-rich solution<br>from FI Conc. | 54 ± 6   | < 231   | < 31       | 3298 ± 142 | 1523 ± 105 | < 31     | 417 ± 39 |

Table 13: Comparison of the concentration of 5 heavy metals present in the P-rich solutions with typical values for P-Rock and future recovered phosphorus salts legislation (Processed results from Table 8)

\*These 7 elements have been studied because they are the one that will be regulated by the European commission for the product from recovered P (Joint Research Centre 2018). Hg is missing but the ICP-MS used was no able to measure it.

\*\*The product after post-treatment of the P-rich solution falls into the category of recovered phosphorus salts as described in a proposal from December 2018 (Joint Research Centre 2018). This document refers to heavy metal limits for future Product Fertilizer Categories (PFC's, in this case, PFC 1(C)1: Inorganic Macronutrient Fertilizer) in a proposed and by EP amended revision of the fertilizer Ordinance. A product containing 35% of P<sub>2</sub>O<sub>5</sub> is considered as reference in the present study which is the minimum phosphate content for this category. The P content is 15.3% of the weight.

\*\*\*Dittrich and Klose 2008 give the typical amount of heavy metals in the P-rock from Morocco, which is taken as an indicator in this study considering that the country holds around 70% of the world P-rock. The phosphorus content of these rocks is taken from Tahib 2015. The P content is 13.9% of the weight.

The heavy metal concentrations in these P-rich solutions were in line with the future legislation on recovered phosphorus salts and the common concentration in P-rock for most of the elements considered (except for Ni in FI Conc. and As in NL Conc.) (Table 13). The analytical method for Cd and Cr needs to be further developed to lower the limit of quantification. Concentrations of organic micro pollutants, macroscopic impurities and pathogens have not yet been considered and this requires further evaluation in the future. The P-rich solution could be used as liquid fertilizer or be further processed by adding Calcium to precipitate calciumphosphate. In addition, the iron hydroxide precipitate could possibly be reused in the steel industry or transformed to iron chloride by dissolution in hydrochloric acid. In the last case, the heavy metals in the iron residue may require removal.

Through the magnetic separation and the alkaline treatment, 16-32% of P has been recovered from the digested sludge. This is a promising result for a first proof of concept, the objective of this study, considering that the digested sludge has not being optimized for maximum vivianite formation. Further optimization is needed to increase the P recovery and make this approach economically relevant. Firstly, the vivianite content in the digested sludge needs to be maximized (which was not the case for the NL sludge). Increasing the Fe dosing could convert 70-90% of the P in the digested sludge into vivianite (Wilfert et al. 2018) which makes it available for magnetic separation. Secondly, recovery and grade can be improved by using a device in which magnetic field and separation matrix can be adjusted (use of rods instead of teeth for instance). The influence of these parameters on the separation efficiency is described in Finch and Wills, 2015.

Not only could this technology allow to recover P as vivianite, but its implementation at WWTP's could reduce the quantity of sludge to dispose of, and increase the heating value of

this waste sludge by decreasing its mineral content. First estimates show that these benefits, especially the expected reduction of the sludge volume, are in balance with the investment and operation costs of a magnetic separator (Wilfert 2018b). Pilot plant operations will have to further confirm the economic benefits of the approach. A direct land application of this sludge with a lower P content would also be easier considering the limitations of P in soil. Finally, a better control of the vivianite precipitation through Fe dosing could minimize the formation of scaling which is a serious problem for WWTP's. These advantages could help making the process economically viable and, therefore, boost the change to a circular economy for P.

## 5. Conclusion

Vivianite is the most prominent P sink in digested sewage sludge and can contain between 70-90% of the total P provided enough iron is present in the sludge. This study proved for the first time the feasibility of the extraction of this mineral with wet magnetic separation technologies. The separated vivianite had a grade of 50-60% and the recovered P-rich solution presented heavy metals concentrations in line with recovered phosphorus legislation. As a proof of concept this is a promising result, but, additional research and development is necessary to improve the P recovery efficiency, for instance through the increase of the Fe dosed to maximize vivianite formation, and the optimization of its magnetic separation from digested sludge.

## 6. Acknowledgments

This work was performed in the TTIW-cooperation framework of Wetsus, European Centre Of Excellence For Sustainable Water Technology ([www.wetsus.nl](http://www.wetsus.nl)). Wetsus is funded by the Dutch Ministry of Economic Affairs, the European Union Regional Development Fund, the Province of Fryslân, the City of Leeuwarden and the EZ/Kompas program of the “Samenwerkingsverband Noord-Nederland”. We thank the participants of the research theme “Phosphate Recovery” for their financial support and helpful discussions. A special thanks goes to Kees Langeveld from ICL Fertilizers who was the first to suggest magnetic separation techniques. We also want to express our gratitude to Peter Berkhout and his co-workers for the amazing work in the development and building of the  $\mu$ -Jones separator. Additionally, we thank Outi Grönfors and Wout Barendregt from Kemira and Stefan Geilvoet from Waterschap Hollandse Delta for valuable support during sludge sampling in Espoo and Dokhaven and for providing valuable information about the treatment parameters of these plants.

## 7. References

- Barrado, E., Prieto F., Ribas J., Lopez F.A. (1999). Magnetic separation of ferrite sludge from a wastewater purification process. *Water air and soil pollution*, 115(1), 385-394.
- Bouderbala, A. (2016). Magnetic separation of vivianite from sewage sludge. Master’s thesis realized at Wetsus in cooperation with the Paris Region Institut for Applied Science (Institut Francilien des Sciences Appliquées).
- Čermáková. Z., Švarcová. S., Hradil. D., Bezdicka. P. (2013). Vivianite: A historic blue pigment and its degradation under scrutiny. *Science and Technology for the Conservation of Cultural Heritage*, 75-78.



Childers, D., Corman, J., Edwards, M., Elser, J. (2011). Sustainability Challenges of Phosphorus and Food: Solutions from Closing the Human Phosphorus Cycle. *BioScience*, 61(2), 117–124.

Cornel, P., Schaum, C., (2009). Phosphorus recovery from wastewater: needs, technologies and costs. *Water Science & Technology*, 59(6), 1069–1076.

Dittrich, B., & Klose, R. (2008). Schwermetalle in Düngemitteln. *Landesamt Für Umwelt, Landwirtschaft Und Geologie*, 3

Egle, L., Rechberger, H., Krampe, J., & Zessner, M. (2016). Phosphorus recovery from municipal wastewater: An integrated comparative technological, environmental and economic assessment of P recovery technologies. *Science of the Total Environment*, 571, 522–542.

Finch, J. and Wills, B.A., (2015). Chapter 13: Magnetic and Electrical Separation. *Wills Mineral Processing Technology, 8<sup>th</sup> Edition*.

Fodoué, Y., Nguetnkam, J. P., Tchameni, R., Basga, S. D., & Penaye, J. (2015). Assessment of the Fertilizing effect of Vivianite on the Growth and yield of the Bean “phaseolus vulgaris” on Oxisoils from Ngaoundere. *International Research Journal of Earth Sciences*, 3(4), 18-26.

Frederichs, T., von Döbeneck, T., Bleil, U., & Dekkers, M. J. (2003). Towards the identification of siderite, rhodochrosite, and vivianite in sediments by their low-temperature magnetic properties. *Physics and Chemistry of the Earth*, 28(16–19), 669–679.

Frossard, E., Bauer, J.P., Lothe, F. (1997). Evidence of vivianite in FeSO<sub>4</sub>-floculated sludges. *Water research*, 31(10), 2449–2454.

Grodzicki, M., Amthauer, G. (2000). Electronic and magnetic structure of vivianite : cluster molecular orbital calculations. *Physics and Chemistry of the minerals*, 27(10), 694–702.

Klencsár, Z. (1997). Mössbauer spectrum analysis by Evolution Algorithm. *Nuclear Instruments and Methods in Physics Research Section B: Beam Interactions with Materials and Atoms* 129(4), 527–533.

Manning, P. G., Murphy, T. P., & Prepas, E. E. (1991). Intensive formation of vivianite in the bottom sediments of mesotrophic Narrow Lake, Alberta. *Canadian Mineralogist*, 29, 77–85.

McCammon, C. A., & Burns, R. G. (1980). The oxidation mechanism of vivianite as studied by Mossbauer spectroscopy. *American Mineralogist*, 65(3–4), 361–366.

Minyuk, P. S., Subbotnikova, T. V., Brown, L. L., & Murdock, K. J. (2013). High-temperature thermomagnetic properties of vivianite nodules, Lake El'gygytyn, Northeast Russia. *Climate of the Past*, 9(1)

Mori, H., & Ito, T. (1950). The structure of vivianite and symplectite. *Acta Crystallographica*, 3(1), 1–6.

Nishihara, Y., & Ogawa, S. (1979). Mössbauer study of  $^{57}\text{Fe}$  in the pyrite-type dichalcogenides-isomer shift of divalent iron in low spin state. *Le Journal de Physique Colloques*, 40(C2).

Nriagu, J. O., & Dell, C. I. (1974). Diagenetic Formation of Iron Phosphates in Recent Lake Sediments. *American Mineralogist*, 59, 934–946.

Poffet, M. S., Käser, K., & Jenny, T. A. (2008). Thermal runaway of dried sludge granules in storage tanks. *CHIMIA International Journal for Chemistry*, 62(1), 29–34.

Recham, N., Armand, M., Laffont, L., Tarascon, J.-M. (2009). Eco-Efficient Synthesis of  $\text{LiFePO}_4$  with Different Morphologies for Li-Ion Batteries. *Electrochemical and Solid-State Letters*, 12(2), A39-44.

Ridder, M., de Jong, S., Polchar, J., Lingemann, S. (2012). Risks and Opportunities in the Global Phosphate Rock Market. PDF document. Available at: [http://www.phosphorusplatform.eu/images/download/HCSS\\_17\\_12\\_12\\_Phosphate.pdf](http://www.phosphorusplatform.eu/images/download/HCSS_17_12_12_Phosphate.pdf)

Consulted on the 06/06/2018

Rombolà, A. D., Toselli, M., Carpintero, J., Quartieri, M., Torrent, J., Marangoni, B. (2007). Prevention of Iron - Deficiency Induced Chlorosis in Kiwifruit (*Actinidia deliciosa*) Through Soil Application of Synthetic Vivianite in a Calcareous Soil, *Journal of plant nutrition*, 26(10-11), 2031-2041.

Rothe, M., Kleeberg, A., & Hupfer, M. (2016). The occurrence, identification and environmental relevance of vivianite in waterlogged soils and aquatic sediments. *Earth-Science Reviews*, 158, 51–64

Rouzies, D., & Millet, J. M. M. (1993). Mossbauer Study of Synthetic Oxidized Vivianite at Room-Temperature. *Hyperfine Interaction.*, 77(1–2), 19–28.

Schoumans, O. F., Bouraoui, F., Kabbe, C., Oenema, O., & van Dijk, K. C. (2015). Phosphorus management in Europe in a changing world. *Ambio*, 44(2), 180–192.

Seitz, A., Riedner, J., Malhotra, K., Kipp, J. (1973). Iron-Phosphate Compound Identification in Sewage Sludge Residue. *Environmental Science and Technology*, 7(4), 354–357.

Taib, M. (2014). The mineral industries of Morocco and western Sahara. *U.S. Geological survey mineral yearbook*, 59.1-59.13

Taylor, K. G., Hudson-Edwards, K. A., Bennett, A. J., & Vishnyakov, V. (2008). Early diagenetic vivianite ( $\text{Fe}_3(\text{PO}_4)_2 \cdot 8\text{H}_2\text{O}$ ) in a contaminated freshwater sediment and insights into zinc uptake: A  $\mu$ -EXAFS,  $\mu$ -XANES and Raman study. *Applied Geochemistry*, 23(6)

Test Methods for Evaluating Solid Waste, Physical/Chemical Methods, EPA publication SW-846, Third Edition, Final Updates V (2015), Method 60-10-D

Van Dijk, K. C., Lesschen, J. P. and Oenema, O. (2016). Phosphorus flows and balances of the European Union Member States. *Science of the Total Environment*, 542, 1078–1093.

Wilfert, P., Kumar, P. S., Korving, L., Witkamp G.J., Van Loosdrecht, M. C. M. (2015). The relevance of Phosphorus and iron chemistry to the recovery of phosphorus from wastewater. *Environmental Science and Technology*, 49(16)

Wilfert, P., Mandalidis, A., Dugulan, A. I., Goubitz, K., Korving, L., Temmink, H., Witkamp G.J., Van Loosdrecht, M. C. M. (2016). Vivianite as an important iron phosphate precipitate in sewage treatment plants. *Water Research*, 104, 449–460

Wilfert, P., Korving, L., Dugulan, I., Goubitz K., Witkamp, G. J., Van Loosdrecht M.C.M. (2018). Vivianite as the main phosphate mineral in digested sewage sludge and its role for phosphate recovery. *Water Research*, 144, 312-321

Wilfert, P. (2018b). Thesis: Phosphate recovery from sewage sludge containing iron phosphate.

Wills, B.A.; Napier-Munn, T.J. (2006). Will's Mineral Processing Technology: An Introduction to the Practical Aspects of Ore Treatment and Mineral Recovery.

Yang, X., Wu, X., Hao, H., He, Z. (2008). Mechanisms and assessment of water eutrophication. *Journal of Zhejiang University SCIENCE B*, 9(3), 197–209.

Zelibor, J. L., Senftle, F. E., & Reinhardt, J. L. (1988). A proposed mechanism for the formation of spherical vivianite crystal aggregates in sediments. *Sedimentary Geology*, 59(1–2), 125–142.

## Appendix A

| WWTP                    | Fe dosing strategy           | Solid Retention Time (days) |         |          | Fe/P molar ratio |                 | Capacity<br>(p.e. in 150g TOC/day) |
|-------------------------|------------------------------|-----------------------------|---------|----------|------------------|-----------------|------------------------------------|
|                         |                              | A-stage                     | B-stage | Digester | Before digestion | After digestion |                                    |
| Dokhaven<br>(AB plant)  | Fe (III) salts in<br>A-stage | 0.3                         | 5.5     | 35       | 0.85             | 1.07            | 564,000                            |
| Espoo<br>(standard CPR) | Fe (II) salts                | 6-10 (1 step)               |         | 13-14    | 2.19             | 2.40            | 321,045                            |

Table A1: Characteristics of the studied WWTP's (data from Wilfert et al. 2017)

The Fe/P molar ratio increases after digestion partly due to extra iron added just before digestion in Dokhaven. For Espoo iron-rich secondary sludge was sampled and combined with primary settled sludge in the digester which explains this increase.

Characteristics of both sludges are given in Table A2: Characteristics of the sieved sludges used in the experiments. It is interesting to notice that the molar Fe/P ratio decreases of ~10% after sieving. The pH has been measured by potentiometry while Total Solid (TS) and Volatile Solid (VS) have been determined following standard methods (APHA, AWWA, WEF 1998). Total P and Fe concentration have been determined by ICP-OES after HNO<sub>3</sub>-assisted microwave digestion.

| Parameter        | Netherland | Finland |
|------------------|------------|---------|
| pH               | 7.6        | 7.3     |
| TS (g/kg sludge) | 22.2       | 24.2    |

|  |       |       |
|--|-------|-------|
| VS (g/kg sludge)                             | 14.1  | 13.8  |
| Total P concentration (mg P/ kg<br>sludge)   | 57.9  | 30.2  |
| Total Fe concentration (mg Fe/ kg<br>sludge) | 103.0 | 119.2 |
| Molar Fe: P ratio                            | 0.99  | 2.19  |

*Table A2: Characteristics of the sieved sludges used in the experiments*

## Appendix B

There are two basic phenomena that determine the separation of magnetic particles from the slurry. First of all, the particles need to reach the teeth as the sludge is poured into the  $\mu$ -Jones, and then they need to stick to it without being dragged by the slurry. In our experiments, the average velocity for particles of 10-100  $\mu\text{m}$  of diameter (hypothesis based on the authors SEM-EDX observations) toward the magnetic plate of the separator is 3 mm/s. This is high enough to reach the teeth for a classic residence time of a few seconds. Secondly, once attached, the particles need to stick to the wall without being dragged by the slurry. By studying the forces applying on a magnetic particle attached to the teeth, it is possible to determine the maximum feeding flow rate to use before detaching them. The following calculations indicate that a flow rate lower than 28.2 mL shouldn't detach vivianite particles bigger than 10 $\mu\text{m}$ .

### Detailed calculations

As the slurry flows along the surface at high magnetic gradient, the paramagnetic particles in the slurry are attracted towards the surface by a force

$$F_{\text{magnetic}} = \mu_0 \rho_p V_p \chi_p H \nabla H \quad (\text{B1})$$

Here,  $\mu_0 = 4\pi \cdot 10^{-7}$  Tm/A is a universal constant of the laws of magnetics,  $H$  (A/m) is the magnetic field and  $\nabla H$  (A/m<sup>2</sup>) is its gradient. The particle is defined by its density  $\rho_p$  (kg/m<sup>3</sup>), its magnetic susceptibility  $\chi_p$  (m<sup>3</sup>/kg) and its volume  $V_p$  (m<sup>3</sup>). As the paramagnetic particles travel towards the surface, they experience a drag force. Since the speed  $\Delta v$  of the particle towards the surface is typically of the order of 1 mm/s or less, and particles are 10-100 micron in diameter, the drag on the particle can be estimated by Stokes' formula:

$$F_{\text{drag}} = 3\pi\eta\Delta v D_p \quad (\text{B2})$$

Here,  $\eta$  (kg/m\*s) is the dynamic viscosity of the slurry and  $D_p$  (m) is the diameter of the particle. Small fines in a liquid very quickly reach a velocity at which drag and external forces are at equilibrium, and so the equations above can be used to estimate  $\Delta v$  for a spherical particle,

$$\Delta v = \frac{\mu_0 \rho_p D_p^2 \chi_p H \nabla H}{18\eta} \quad (\text{B3})$$

Magnetic susceptibilities of Vivianite nodules were found to vary in the range from 0.8 to 1.7  $10^{-6}$  m<sup>3</sup>/kg by Minyuk et al. 2013. Conservatively assuming the lower value, a density for Vivianite of 2300 kg/m<sup>3</sup>, and a viscosity of the slurry of twice that of water, 2  $10^{-3}$  kg/m.s, the speed of 10 micron diameter Vivianite particles towards the surface can be estimated as

$$\Delta v = 6 \cdot 10^{-18} \text{ A}^{-2} \text{ m}^4 \text{ s}^{-1} H \nabla H \quad (\text{B4})$$

Target slurries contain organic fibers of up to 1mm length and so the channels for the slurry should leave at least a space of 2 mm between surfaces to avoid blocking. Still, this means that an average field of  $10^6$  A/m and an average field gradient of  $0.5 \cdot 10^9$  A/m<sup>2</sup> (i.e. varying by  $0.5 \cdot 10^6$  A/m over 1 mm from the center of the channel towards the surface) would result in a particle speed of 3 mm/s. This is more than enough for all such particle to reach the surface for a typical residence time of one or more seconds. Field conditions like these do not require superconducting magnets or steel wool. They can be met by Jones separators with electromagnets and grooved plates, which has the advantage of low investment cost and simple channel geometries that do not easily block.

Once the magnetic particles have reached the surface, they should stick there and not be carried along the surface by the drag of the slurry. The Reynolds number of the flow in the channels formed by the surface is typically below 100, so the friction of the slurry flow per unit area of the coating of magnetic particles on the surface of the channels is



$$f_{\text{friction slurry}} = \frac{8\eta v}{D} \quad (\text{B5})$$

Here  $v$  (m/s) is the velocity of the slurry past the surface and  $D$  (m) is the diameter of the channel. The friction of the surface of a particle is proportional to the magnetic force pulling the particle to the surface:

$$F_{\text{friction surface}} = fF_{\text{magnetic}} = f\mu_0\rho_p V_p \chi_p H \nabla H \quad (\text{B6})$$

Since  $F_{\text{friction surface}} > A_p f_{\text{friction slurry}}$ , where  $A_p$  is the part of the surface covered by a single particle, the magnetic field should be strong enough to fix the magnetic particles to the surface:

$$H \nabla H > \frac{8\eta A_p v}{f\mu_0\rho_p V_p \chi_p D} \quad (\text{B7})$$

Taking again the values for Vivianite as above, and estimating  $f=0.5$ , while conservatively taking  $A_p = 5D_p^2$ , we get:

$$H \nabla H > 1.7 \cdot 10^{15} \text{ A}^2 \text{ m}^{-4} \text{ s}^1 v \quad (\text{B8})$$

With  $v \approx 0.1$  m/s, this means that, again, Jones separators will do well.

For a full coating of particles  $A_p = 5D_p^2$ , is a very conservative estimate, since it would be expected that each particle covers roughly its square diameter of the surface. However, for a single particle sticking from the surface, this estimate is probably more appropriate.

| Total flow<br>mL/min | Drag + gravity force on particles near the wall (pN) |                  |                  | Magnetic stick force on the wall (pN) |                  |                  |
|----------------------|--|------------------|------------------|---------------------------------------|------------------|------------------|
|                      | 10 $\mu\text{m}$                                     | 20 $\mu\text{m}$ | 30 $\mu\text{m}$ | 10 $\mu\text{m}$                      | 20 $\mu\text{m}$ | 30 $\mu\text{m}$ |
| 7.8                  | 45   | 207              | 525              | 142                                   | 1130             | 3820             |
| 16.2                 | 83   | 360              | 869              | 142                                   | 1130             | 3820             |
| 24.0                 | 122  | 513              | 1210             | 142                                   | 1130             | 3820             |
| 32.4                 | 160  | 666              | 1560             | 142                                   | 1130             | 3820             |

|      |     |     |      |     |      |      |
|------|-----|-----|------|-----|------|------|
| 40.2 | 198 | 819 | 1900 | 142 | 1130 | 3820 |
|------|-----|-----|------|-----|------|------|

Table B1: Forces applying on vivianite depending on the flow rate

| Total flow<br>mL/min | Ratio of drag and stick |                  |                  |
|----------------------|-------------------------|------------------|------------------|
|                      | 10 $\mu\text{m}$        | 20 $\mu\text{m}$ | 30 $\mu\text{m}$ |
| 7.8                  | 0,32                    | 0,18             | 0,14             |
| 16.2                 | 0,59                    | 0,32             | 0,23             |
| 24.0                 | 0,86                    | 0,45             | 0,32             |
| 32.4                 | 1,13                    | 0,59             | 0,41             |
| 40.2                 | 1,40                    | 0,72             | 0,50             |

Table B2: Ratio of the drag and stick forces depending on the flowrate

Under all these assumptions, it can be seen in Table B2: Ratio of the drag and stick forces depending on the flowrate that a flow rate lower than 24 mL/min should allow all the particles  $>10 \mu\text{m}$  to stick to the walls of the  $\mu$ -Jones (ratio  $<1$ ). The exact cut-off for these particles is 28.2 mL/min.

#### Viability of magnetic separation

Experiments were performed to test the viability of magnetic separation of vivianite from sludge. The four tested flow rates are lower than the 28.2 mL/min cut-off previously determined to be sure that the separation will work and to also separate particles smaller than  $10 \mu\text{m}$ . The separation protocol was the same as described in the Material & Methods section with the difference that the flow rate varied and that the pouring time was 30 seconds for both sludges.

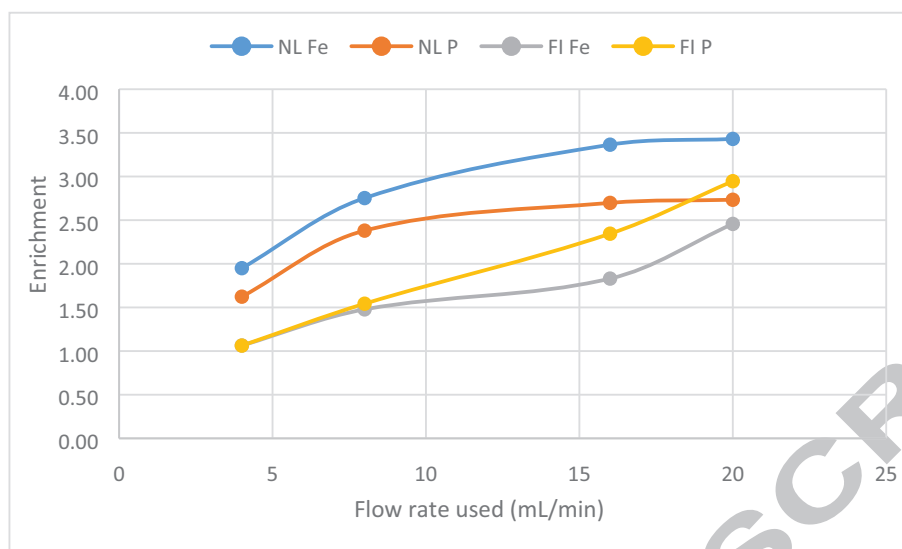


Figure B1: Enrichment for P and Fe for both sludge at four different flow rates (The enrichment defines the ratio of the weight content of a Fe and P before and after magnetic separation)

First of all, the separation works for flowrates below 20 mL/min which is in the expected range obtained by theoretical modeling. Indeed, from a certain flow rate, the drag force exerted by the slurry on a particle stuck on the surface becomes higher than the one retaining it against the wall. Figure 3 shows that for both sludges the enrichment increases for both Fe and P with the flow rate. This is in line with the expectations since non-magnetic impurities are more likely to be flushed out at higher flow rates. The enrichment shows a saturation around 20 mL/min for the Dutch sludge which is not the case for the Finnish sludge (Table B1: Forces applying on vivianite depending on the flow rate). The maximum magnetic species may have been extracted from the Dutch sludge while a longer pouring time may be needed for the Finnish sludge. It is in accordance with the higher Fe/P ratio of the Finnish sludge, suggesting that a bigger magnetic fraction, containing siderite ( $\text{FeCO}_3$ ), pyrite or/and  $\text{FeO}$ 's, is present.

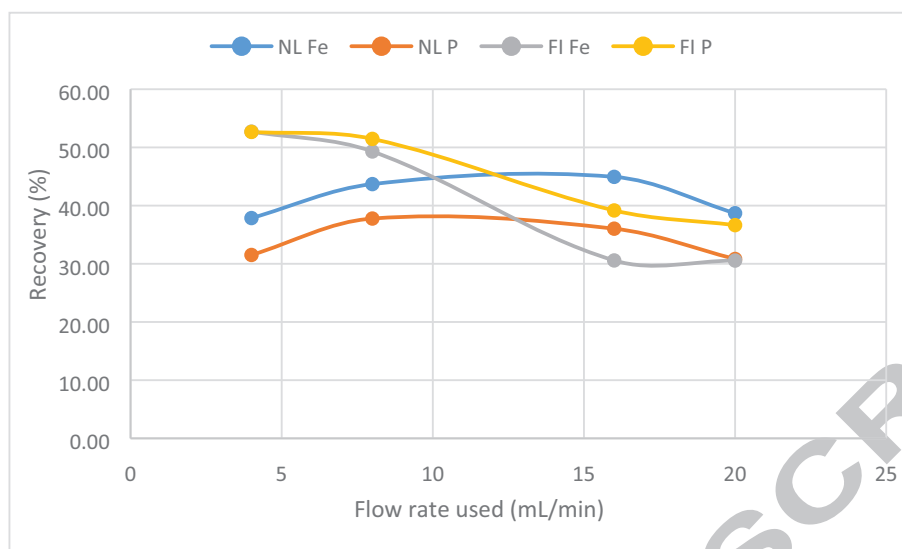


Figure B2: Recovery of P and Fe for both sludge at four different flow rates

Aside from the enrichment, the recovery of P and Fe has been measured as well. The recovery decreases with the flow rate for the Finnish sludge for both elements while it remains rather stable for the Dutch feed (Table B2: Ratio of the drag and stick forces depending on the flowrate). Higher streams reduce the part of non/less-magnetic material susceptible to be retained which explains the behavior of the Finnish sludge. 20 mL/min was the highest flow rate tested and, even though it gave lower recovery, it gave the purest product with lower organic matter content and impurities like calcium, sulfur, and silicon. Determining the quantity of vivianite present in the concentrate is easier with purer sample. Therefore, 20 mL/min have been chosen as the working flow rate.

## Reference

Minyuk, P. S., Subbotnikova, T. V., Brown, L. L., & Murdock, K. J. (2013). High-temperature thermomagnetic properties of vivianite nodules, Lake El'gygytgyn, Northeast Russia. *Climate of the Past*, 9(1)

## Appendix C

### Carbonate determination

The carbonate content in the sample has been estimated using  $\mu$ GC. First, 20 mg of solid is added to a 25 mL glass vial. 1 mL of HCl 9% (VWR Chemicals) is quickly poured on the powder, and the jar is immediately closed with a rubber stopper. After 10 minutes, 10 mL of the gas phase is withdrawn and quickly introduced in a  $\mu$ GC for CO<sub>2</sub> determination. The device is a Varian CP 4900 equipped with a Thermal Conductivity Detector. The column used is a PoraPlot U of 10 m long with Helium as a carrier. The data processing is realized with the software GC solution. A blank without any solid but only acid was also prepared.

The quantity of CO<sub>2</sub> released and the quantity of carbonate in the samples are presented in Table C1: Percentage of carbon dioxide evolution and FeCO<sub>3</sub> content assuming all evolved carbon dioxide was associated to FeCO<sub>3</sub> (calculation below). There is significantly more carbonate in the samples from Finland (3-5% of dried solid) than the one from the Netherlands (< 1%). Independently from the sludge origin, the share of carbonate seems to decrease after magnetic separation. No CO<sub>2</sub> release has been observed in the case of the scaling sample.

| Sample   | X <sub>CO2</sub> (%) | X <sub>FeCO3</sub> (%) |
|----------|----------------------|------------------------|
| Blank    | 0.06                 | 0.00                   |
| FI Feed  | 1.33 ± 0.01          | 4.94 ± 0.04            |
| FI Conc. | 0.95 ± 0.03          | 3.33 ± 0.16            |
| NL Feed  | 0.25 ± 0.01          | 0.60 ± 0.03            |
| NL Conc. | 0.13 ± 0.01          | 0.26 ± 0.02            |
| Scaling  | 0.06                 | 0.00                   |

*Table C1: Percentage of carbon dioxide evolution and FeCO<sub>3</sub> content assuming all evolved carbon dioxide was associated to FeCO<sub>3</sub>*

ACCEPTED MANUSCRIPT

Hypothesizing the total reaction  $\text{FeCO}_3 + 2\text{HCl} \rightarrow \text{FeCl}_2 + \text{H}_2\text{O} + \text{CO}_2$ , the determination of the carbonate fraction can be done as follow:

$$n_{\text{CO}_2} = \frac{(X_{\text{CO}_2} - X_0) \times \rho_{\text{air}} \times V_{\text{gas}}}{M(\text{CO}_2)} \quad (\text{C1})$$

1 mole of  $\text{FeCO}_3$  releases 1 mole of  $\text{CO}_2$  so:

$$n_{\text{CO}_2} = n_{\text{FeCO}_3} \quad (\text{C2})$$

Giving finally:

$$X_{\text{FeCO}_3} = \frac{n_{\text{FeCO}_3} \times M(\text{FeCO}_3)}{m_{\text{sample}}} \quad (\text{C3})$$

With:

$n_{\text{CO}_2}$  the amount of substance of  $\text{CO}_2$  released in the tube in moles

$X_{\text{CO}_2}$  the  $\text{CO}_2$  weight fraction of the gaseous phase in the tube

$X_0$  the  $\text{CO}_2$  weight fraction of the blank

$\rho_{\text{air}}$  the density of air worth 1.20 g/L at the experimental conditions (20°C at sea level)

$V_{\text{gas}}$  the total volume of the gaseous phase in the tube worth 0.0240 L (1 mL of HCl in 25 mL tube)

$M(\text{CO}_2)$  the molar weight of  $\text{CO}_2$  worth 44.0 g/mol

$n_{\text{FeCO}_3}$  the amount of substance of  $\text{FeCO}_3$  in the sample in moles

$X_{\text{FeCO}_3}$  the  $\text{FeCO}_3$  weight fraction of the solid

$M(\text{FeCO}_3)$  the molar weight of  $\text{FeCO}_3$  worth 115.8 g/mol

$m_{\text{sample}}$  the weight of the sample introduced into the tube in g

#### Quartz determination

It has been noticed that when a sufficient quantity (50 mg) of feed or concentrate is digested, an insoluble white solid remains. Quartz ( $\text{SiO}_2$ ) is hard, or even impossible, to degrade with standard acid digestion. The solid fraction remaining after digestion was carefully collected by centrifugation and dried at 105 °C.

The undigested solid after digestion was isolated and analyzed by SEM-EDX. Si and O were the main components of the sample (>80% of total weight) in a ratio close to the one of  $\text{SiO}_2$ . However, there were some other elements homogeneously distributed ranging from Na, Al and Ca at high concentration, to Fe, P, and Cu at minor concentration. The dry weight of the digestion residue was assumed to be entirely quartz for the calculations (Table C2: Digestion residue (assumed to be quartz) content in both sludges

| Sample   | Average (% of vacuum dried matter) |
|----------|------------------------------------|
| FI Feed  | 8                                  |
| FI Conc. | 8                                  |
| NL Feed  | 4                                  |
| NL Conc. | 7                                  |

Table C2: Digestion residue (assumed to be quartz) content in both sludges



## Appendix D

The analytical method chosen for each element as well as the isotope measured is the one recommended by the supplier (Table D1: Isotopes analyzed and corresponding methods according to standard settings). When gases are used, they are introduced through the skimmer cone (iCRC system) and not in a reaction chamber which is usually the case. Sample collection was done by a FAST 4DX autosampler, from supplier ESI, combined with a FAST collection loop of 1 ml. This allowed rinsing of the uptake tubes, while the sample was simultaneously analyzed from the loop. All the sample, as well as the rinse solution, were prepared with ultra-pure HNO<sub>3</sub> from Fluka and the sample with ultra-pure water from Sigma-Aldrich. The acid content was 4% for all solutions to increase the concentration of traces elements at a maximum. Together with the samples, a blank is prepared by digesting a sample of ultra-pure water only, in the same temperature and acid conditions than with solid sample.

The calibration curve was realized with standard solutions from Perkin Elmer in 3 different solutions (Table D2: Composition of the standard solutions used for calibration of the ICP-MS) and the concentration used were 0.1/1/5/10/25/50 ppb. These solutions have been prepared in low range to study the elements which concentration cannot be attained with simple ICP-OES. More concentrated elements are not determined here. Result accuracy was checked by analyzing standard reference material 1640a (supplier NIST) at the start and end of the run. The software used for data processing was Aspect MS 4.3.

According to the high NaOH background in the release solution, the samples need to be diluted not to damage the devices. A final concentration of 225 ppm of Na is set to be below the maximum amount of salt allowed of 1000 ppm. The protocol for the experiments stays the same, but with a blank of 225 ppm of Na prepared with ultra-pure water and NaOH. No particular calibration curve has been prepared for samples with NaOH background.

| Analytical mode | Isotope analyzed  |
|-----------------|---|
| H <sub>2</sub>  | <sup>52</sup> Cr, <sup>75</sup> As, <sup>78</sup> Se, <sup>133</sup> Cs, <sup>139</sup> La  |
| He              | <sup>23</sup> Na, <sup>56</sup> Fe, <sup>85</sup> Rb, <sup>140</sup> Ce   |
| ng              | <sup>7</sup> Li, <sup>9</sup> Be, <sup>11</sup> B, <sup>24</sup> Mg, <sup>27</sup> Al, <sup>29</sup> Si, <sup>31</sup> P, <sup>34</sup> S, <sup>39</sup> K, <sup>44</sup> Ca, <sup>47</sup> Ti,<br><sup>55</sup> Mn, <sup>59</sup> Co, <sup>60</sup> Ni, <sup>65</sup> Cu, <sup>66</sup> Zn, <sup>95</sup> Mo, <sup>107</sup> Ag, <sup>114</sup> Cd,<br><sup>118</sup> Sn, <sup>137</sup> Ba, <sup>205</sup> Tl, Pb |

Table D1: Isotopes analyzed and corresponding methods according to standard settings

| Standard solution | Elements present   |
|-------------------|--|
| 1                 | Ag, Li, Mo, Si, Sn, Tl   |
| 2                 | As, B, P, S, Se  |
| 3                 | Al, Ba, Be, Ca, Cd, Ce, Co, Cr, Cs, Cu, Fe, K, La,<br>Mg, Mn, Na, Ni, Pb, Rb, Zn |

Table D2: Composition of the standard solutions used for calibration of the ICP-MS

## Appendix E

| Sample      | Weight content (g element/kg of P) |                |                |                |             |                |                |                |                |                 |    |               |
|-------------|------------------------------------|----------------|----------------|----------------|-------------|----------------|----------------|----------------|----------------|-----------------|----|---------------|
|             | Cr                                 | As             | La             | Li             | Mg          | Al             | Mn             | Co             | Ni             | Cu              | Cd | Ca            |
| FI Feed     | 1.17<br>±0.02                      | 0.31<br>± 0.02 | 1.06<br>± 0.01 | 0.13<br>± 0.01 | 141<br>± 4* | 215<br>± 4*    | 8.86<br>± 0.02 | 0.31<br>± 0.01 | 1.17<br>± 0.01 | 13.31<br>± 0.15 | nd | 940<br>± 21 * |
| FI Conc.    | 0.39<br>± 0.07                     | 0.12<br>± 0.01 | 0.38<br>± 0.01 | 0.05<br>± 0.01 | 43<br>± 2*  | 71<br>± 2*     | 6.42<br>± 0.05 | 0.14<br>± 0.01 | 6.17<br>± 0.02 | 15.48<br>**     | nd | 265<br>± 10*  |
| NL Feed     | 1.36<br>± 0.02                     | 1.07<br>± 0.03 | 0.25<br>± 0.01 | 0.10<br>± 0.01 | 91<br>± 3*  | 160<br>± 3*    | 17.0<br>± 0.12 | 0.16<br>± 0.01 | 1.13<br>± 0.01 | 18.34<br>± 0.29 | nd | 968<br>± 19*  |
| NL<br>Conc. | 0.77<br>± 0.02                     | 0.23<br>± 0.01 | 0.09<br>± 0.01 | 0.05<br>± 0.01 | 97<br>± 2*  | 60<br>± 2*     | 31.09<br>**    | 0.11<br>± 0.01 | 1.17<br>± 0.01 | 9.20<br>± 0.05  | nd | 259<br>± 6*   |
| Scaling     | nd                                 | nd             | nd             | nd             | 91<br>± 1*  | 2.50<br>± 0.01 | 25<br>± 1*     | 0.27<br>± 0.01 | 0.66<br>± 0.01 | 0.14<br>± 0.01  | nd | 80<br>± 5*    |

Table E1a: Elemental composition of the feeds, concentrates and scaling measured by ICP-MS/OES

nd: no data, meaning below LOQ of both ICP

er.: the ICP-MS device gave an inexplicable error

\* results from ICP-OES

\*\* results from ICP-OES with the element found only in one replicate

| Sample   | Weight content (g element/kg of P) |                |                |                |                 |                |                  |             |              |             |                |                |
|----------|------------------------------------|----------------|----------------|----------------|-----------------|----------------|------------------|-------------|--------------|-------------|----------------|----------------|
|          | Zn                                 | Mo             | Ag             | Sn             | Ba              | Pb             | Na               | Si          | K            | S           | Rb             | Ce             |
| FI Feed  | 25.51<br>± 0.38                    | 0.21<br>± 0.01 | 0.10<br>± 0.01 | 0.96<br>± 0.01 | 4.02<br>± 0.02  | 0.54<br>± 0.01 | 106.91<br>± 1.72 | 278<br>± 4* | 380<br>± 11* | 303<br>± 4* | 0.37<br>± 0.01 | 2.63<br>± 0.03 |
| FI Conc. | 6.42<br>± 0.01                     | 0.06<br>± 0.01 | nd             | 0.24<br>± 0.01 | 1.46<br>± 0.01  | 0.13<br>± 0.01 | nd               | 85<br>± 4*  | 30.96<br>**  | 93<br>± 13* | 0.1<br>± 0.01  | 0.80<br>± 0.01 |
| NL Feed  | 35<br>± 3*                         | 0.32<br>± 0.01 | 0.19<br>± 0.01 | 0.68<br>± 0.01 | 10.73<br>± 0.03 | 3.03<br>± 0.05 | 192.51<br>**     | 187<br>± 3* | 275<br>± 3*  | 558<br>± 6* | 0.21<br>± 0.01 | 0.35<br>± 0.01 |
| NL Conc. | 8.39<br>± 0.09                     | 0.07<br>± 0.01 | 0.04<br>± 0.01 | 0.23<br>± 0.01 | 3.11<br>± 0.02  | 1.05<br>± 0.01 | 3.1<br>± 0.53    | 72<br>± 2*  | 23.32<br>**  | 124<br>± 6* | 0.06<br>± 0.01 | 0.15<br>± 0.01 |
| Scaling  | 2.25<br>± 0.02                     | nd             | nd             | nd             | nd              | 0.03<br>± 0.01 | nd               | nd          | nd           | 14<br>± 7*  | nd             | nd             |

Table E1b: Elemental composition of the feeds, concentrates and scaling measured by ICP-MS/OES

nd: no data, meaning below LOQ of both ICP

er.: the ICP-MS device gave an inexplicable error

\* results from ICP-OES

\*\* results from ICP-OES with the element found only in one replicate

## Appendix F

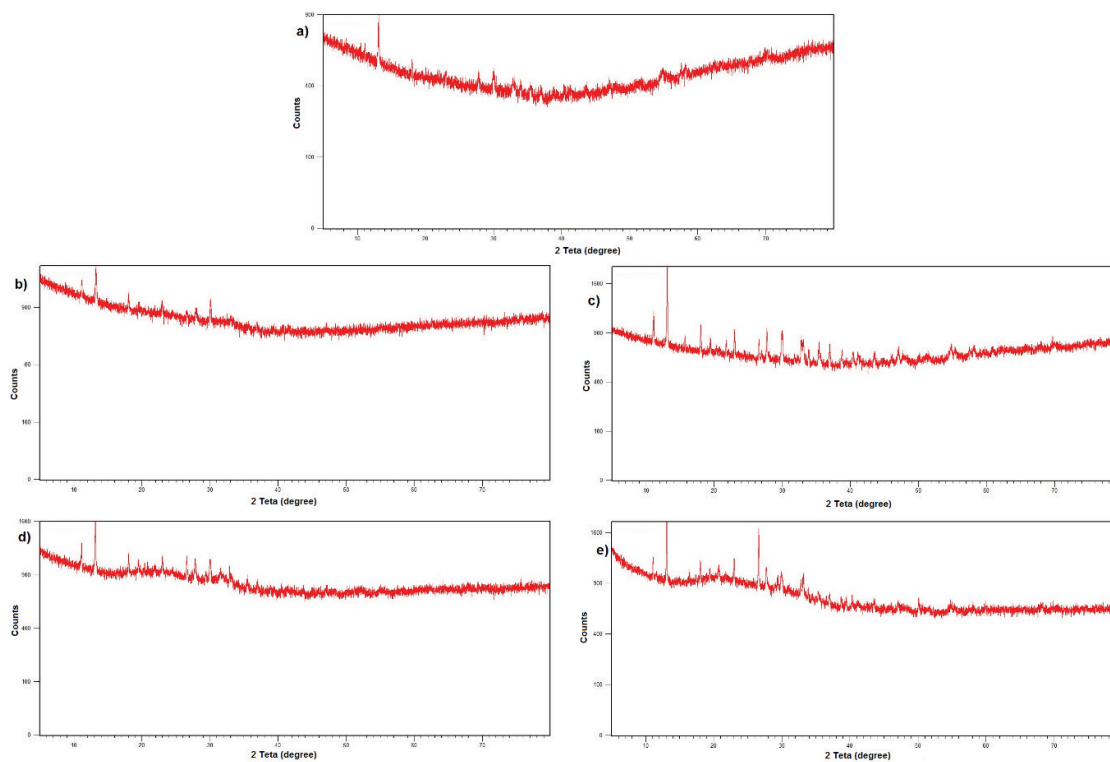
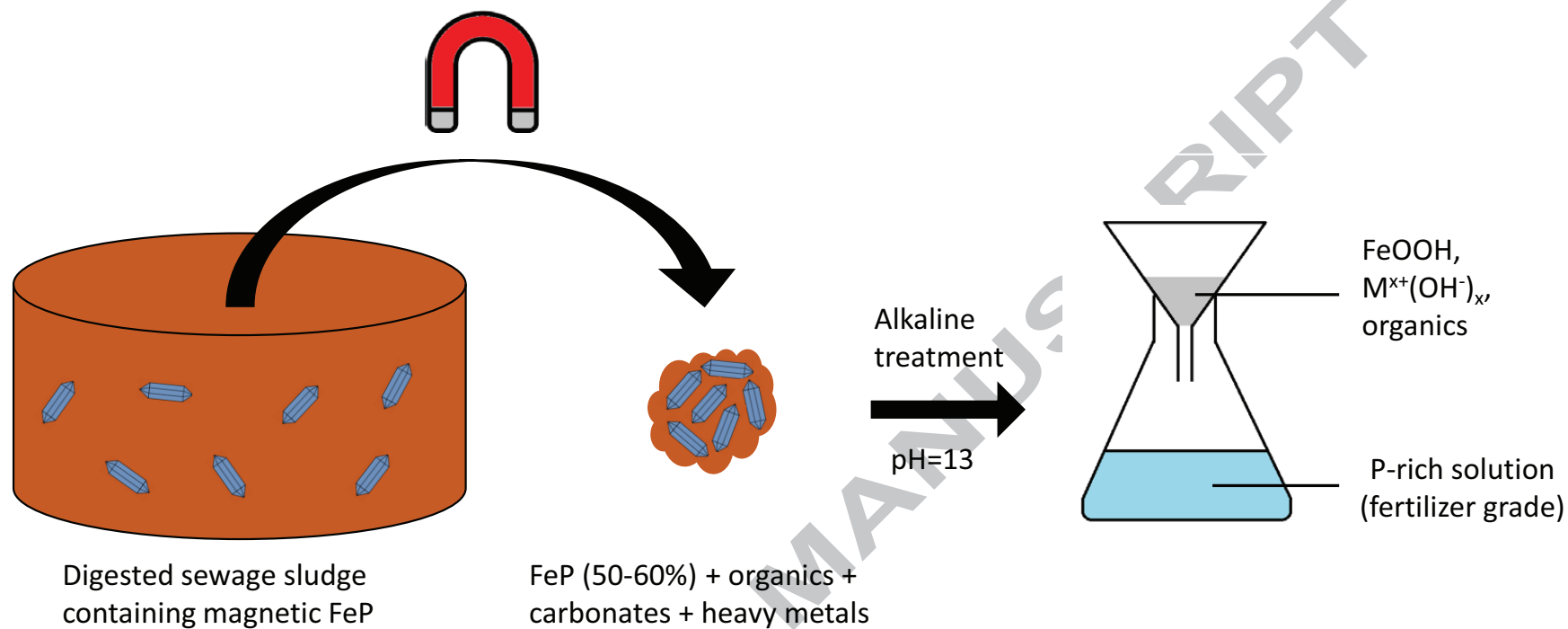


Figure F1: XRD diffractogram for a) the scaling, b) Conc. FI, c) Conc. NL, d) Feed FI and e) Feed NL



### Highlights

- For the first time, vivianite was separated from sludge via a wet magnetic technique.
- The study focuses on the analysis of the extracted vivianite and recovered P.
- The product contains vivianite (50-60%), organic matter (20%), quartz and siderite.
- Phosphorus was recovered and purified from vivianite through alkaline treatment.
- After purification, heavy metals are in line with P rock and future legislation.

ACCEPTED MANUSCRIPT